Interactive comment on "Observational evidence of moistening the lowermost stratosphere via isentropic mixing across the subtropical jet" by J. Langille et al.

Overall Author Response:

Thank you very much for your comments and suggestions regarding our manuscript. We agree with most your suggested changes and have included several edits to the final manuscript that reflect these changes. We believe that the associated changes and additional analysis provides better context for the observations and makes for a more complete paper. We have responded directly to your comments below in red (A.1.#) and have identified where the corresponding changes have been made in the manuscript. In addition to these changes, there have been several format and structural changes that were made to the manuscript in response to suggestions and comments from the second reviewer. Please refer to the responses to the second reviewer for a description of those changes. Note that several new Figures have been added to the manuscript in order to expand the analysis. We have also edited the figures to have the same colormap throughout the paper.

Summary of key revisions made to the paper:

1) A synoptic scale meteorological analysis is included for the Rossby wave breaking event that resulted the observed dynamical structure.
2) Discussion of the process-consistency despite the specific differences between SHOW water vapor structure and the ERA5 dynamical field is made to clarify that multiple factors can contribute to the specific differences, including the physical factor that when wave breaking result in irreversible mixing, the air mass composition loses its correlation with PV as a dynamical tracer.
3) More focused in the objectives and take-home messages of this paper to present the new observational evidence of water vapor transport into lowermost stratosphere driving by Rossby wave breaking and instrument capability and potential impact on stratospheric water vapor budget. Eliminated the additional discussions on the scale of the event and further dynamical analysis to avoid distracting from the main messages.
4) The abstract has also been edited accordingly

Anonymous Referee #1 Received and published: 6 January 2020

The authors present results from a new remote sensing instrument designed for satellite-borne high-vertical resolution limb soundings of water vapor in the upper troposphere/lower stratosphere. The instrument was mounted on board a high-altitude research aircraft and a single cross section obtained of an intrusion of tropospheric air into the lower most stratosphere, just above the subtropical jet is presented. The cross section provides evidence of a moist filament of tropospheric air being mixed poleward into the lower most stratosphere.

Such events are of physical and climatic interest given the role of these events in moistening the extratropical lower stratosphere and thus determining water vapor concentrations in a region important for climate forcing. The observations reveal features at very fine vertical length scales (< 1 km) which are

difficult to observe and to model, although the MLS observations do seem to capture the filament in question to some extent. This filament of elevated water vapor coincides with the (upper) tropopause near the 400 K isentropic surface. The authors suggest tentatively that there may be a bias in the ECMWF reanalysis in the form of a vertical offset of the dynamical fields, in that there is a similarly located region of low potential vorticity air somewhat lower in altitude.

Regardless of this suggestion, this observation of a fine filamentary structure extending into the lowermost stratosphere is certainly worthy of publication, but since the scope of the paper is, as set out by the authors, primarily to present the scientific value in these test observations (not simply to validate them) I think it is appropriate to ask for a bit more follow up analysis on some of the details.

Author Response (A.1.1)

We agree with your request to present some follow up analysis that serves to highlight the scientific value of the SHOW measurements. Therefore, we have added several new Figures (Figure 1- 4) and further analysis of the meteorological fields that provides evidence that the observed moist filament is due to isentropic mixing following a Rossby wave breaking event in the days preceding the ER-2 flight. This is discussed in more detail in A.1.3 below. We have also expanded the discussion in section 6 to examine potential errors in the SHOW measurements, the determination of the upper and lower boundary of the retrieval and reasons for potential biases between SHOW, MLS and the reanalysis data. It also emphasizes the spatial structures in the PTLR in the context of the new analysis of the meteorological fields in support of the suggestion that the moist filament is of tropospheric origin (tropospheric intrusion).

Firstly, the newer ERA 5 reanalysis should be used instead of ERA Interim. It has substantially higher vertical and horizontal resolution, and the data is easily available. It would be also worth looking at model level data which is much finer than the data provided on the 37 pressure-level grid. I am not convinced of the inferred vertical (see below), but in any case, the comparison would be much more relevant in the context of the more modern product.

Author Response (A.1.2)

We are actually using ERA 5, not ERA-interim. The data is provided in 1-hour time steps on a 0.25-degree x 0.25-degree grid. However, the ERA5 products available to us, unfortunately, still has 37 level, with corresponds to 25 hPa vertical resolution in the tropopause region. This is much coarser than the measurement.

Secondly, emphasis has been placed on the vertical and meridional structure of this filament, but the only synoptic details we are given is in the form of an isobaric wind map at 175 hPa. It could be very enlightening to see some maps of potential vorticity on the 400 K and the 380 K isentropic surfaces with a domain comparable to Figure 1, in order to distinguish the filament from the layer of air between the double tropopause structures highlighted in Fig. 3a. These may have quite different horizontal structures that could shed light on the fine vertical structure of the observed water vapor. On a related note, I don't think the text includes a discussion of the line-of-sight resolution of the measurements (i.e. in the longitudinal direction in the current geometry).

Author Response (A.1.3)

In order to address your first point, we have included several additional Figures and associated analysis that we believe provides the necessary context for the case study that is presented in the paper. We have added several paragraphs to Section 3 that discusses these Figures.

Specific changes:

1. We have included a new figure (Figure 2) showing 3 - 48-hour time steps (each day at 20:00 UTC) of PV on the 380 K surface for the 6 days leading up to the date of the case study. The Figure clearly shows a Rossby wave-breaking event has occurred in the days preceding the flight that results in mixing along the subtropical jet.

2. We have added a new figure (Figure 3) shows the PV on the 380 K (Figure 3 (a)) and 400 K (Figure 3 (b)) surfaces for the 07/21/2017 18:00 UTC time step. In the Figures, the tropospheric and stratospheric air masses are separated by the 6PVU contour on the 380 K surface and 8 pvu on the 400 K surface. Here it is observed that the mixing associated with the Rossby wave breaking results in a long low PV "tongue" consistent with tropospheric air that extends from the Western Pacific and tracks the subtropical jet across North America.

3. To characterize the vertical structure we have included a Figure (now Figure 4) that shows the height of the thermal tropopause and the location/extent and height of the secondary tropopause for the 07/21/2017 18:00 UTC time step. In these figures one can clearly see that there are several double tropopause regions located on the poleward of the subtropical jet. The SHOW measurements track crosses one of these regions. While additional time steps are not shown, it is useful to point out that the regions of double tropopause vary in extent from time-step to time-step. In fact, the double tropopause region that SHOW crosses becomes larger near the 21:00 UTC time step. A paragraph has been included in the text that discusses this Figure. We believe that the updated analysis provides the relevant context for the case study and justifies the suggestion that the moist filament observed along the second tropopause in Figure 6 (a) is likely of tropospheric origin.

4. Regarding the line of sight resolution in the longitudinal direction, the SHOW instrument averages over 4 degrees in the horizontal by making use of anamorphic input optics. Therefore, no horizontal scene information is obtained. A sentence has been added after the second sentence of the second paragraph in Section 2 to clarify this point for the reader.

With regards to the suspected offset in the reanalysis output, this is certainly a difficult region to capture correctly and so it seems plausible to me that such an offset could exist. However, it's also possible that the water vapor transport is not aligned with the lowest PV anomaly, or that the layer of most effective intrusion is not where the PV gradients are strongest (after all the meridional PV gradients act as a horizontal mixing barrier that discourages such intrusions). The requested figures should provides some clarity on this point. A related dynamical point is that the potential temperature lapse rate is not a

materially conserved quantity, while PV is (up to diabatic processes); this point should probably be stressed more clearly in the text.

Author Response (A.1.4)

The text has been updated to be clearer on this point. Specifically, the lines highlighting a potential bias between the reanalysis and observations have been removed; however, the identification of the misalignment between the two is discussed. Several new paragraphs have been added to Section 5 that examine the PV and layered thermal structure in the context of mixing following the Rossby wave breaking. It is clarified that it is physically possible (and reasonable) that the dynamical field and chemical structure are no longer intact, which is a sign of an irreversible transport. In addition, the ERA5 products are given at a much coarser resolution than the SHOW measurements. We include a paragraph in the discussion of Section 6 that clarifies these points.

One final minor comment: on line 168 reference is made to orange contours in Figure 3 that I think are in fact dark gray; the orange contours only show up in Figure 4.

Author Response (A.1.5)

The text has been modified so the appropriate "grey" contour is mentioned.

Interactive comment on "Observational evidence of moistening the lowermost stratosphere via isentropic mixing across the subtropical jet" by J. Langille et al.

Anonymous Referee #2 Received and published: 10 January 2020

Overall Author Response:

Thank you very much for your comments and suggestions regarding our manuscript. We agree with most your suggested changes and have included several edits to the final manuscript that reflect these changes. We believe that the associated changes and additional analysis provides better context for the observations and makes for a more complete paper. We have responded directly to your comments below in red (A.2.#) and have identified where the corresponding changes have been made in the manuscript. In addition to these changes, there have been several format and structural changes that were made to the manuscript in response to suggestions and comments from the first reviewer. Please refer to the responses to the first reviewer for a description of those changes. Note that several new Figures have been added to the manuscript in order to expand the analysis. We have also edited the figures to have the same colormap throughout the paper.

Summary of key revisions made to the paper:

1) A synoptic scale meteorological analysis is included for the Rossby wave breaking event that resulted the observed dynamical structure.

2) Discussion of the process-consistency despite the specific differences between SHOW water vapor structure and the ERA5 dynamical field is made to clarify that multiple factors can contribute to the specific differences, including the physical factor that when wave breaking result in irreversible mixing, the air mass composition loses its correlation with PV as a dynamical tracer.
3) More focused in the objectives and take-home messages of this paper to present the new observational evidence of water vapor transport into lowermost stratosphere driving by Rossby wave breaking and instrument capability and potential impact on stratospheric water vapor budget. Eliminated the additional discussions on the scale of the event and further dynamical analysis to avoid distracting from the main messages.
4) The abstract has also been edited accordingly

In this manuscript, the authors present the analysis of a double tropopause-intrusion event as a case study to validate the new SHOW instrument. The authors compare their results to reanalysis and satellite data. I find the work here presented exciting, and no doubt, it lets to get some insight on the potential of the instrument. I want to congratulate the authors for the work developed. At the same time, I have to say that I have detected several mistakes along with the manuscript and that I think that both the analysis and the presentation can be and should be improved. I am familiar with the topic here discussed, and I have found the description sometimes confusing and incomplete. Therefore, those not so familiar with the matter could find it challenging to understand some issues.

One of the more puzzling issues that I have found in the manuscript is that the Introduction is poor in number and the use of appropriate references. There are some striking examples along with the paper because they involve some of the coauthors. This lack of adequate references makes the discussion about the case study not well balanced and can complicate the reader to have a general perspective of the phenomenon. Below I address this issue with some suggestions where it corresponds.

For example, in the first paragraph of the Introduction, it would be appropriate to cite a work that supports the statement on the limitation of models. Sections 6.2.4 and 6.3 of Gettelman et al. (2010) deal with it (https://doi.org/10.1029/2009JD013638). Also, it is usual to cite Gettelman and Forster (2002) when you refer to the CPT (line 37)(https://doi.org/10.2151/jmsj.80.911). The physical mechanisms mentioned (line 54) are well explained with a model and radiosonde data by Ferreira et al. (2015) (https://doi.org/10.1002/qj.2697). It provides an excellent discussion of some of the most relevant constraints, and it would be worthy of citing it to let the reader get some insight on them.

In lines 57-61, the authors discuss the limitations of satellite data. Indeed, they use AURA-MLS for comparison purposes here. I think that they should cite the works validating WV profiles of AURA-MLS for the SPARC Data Initiative, as they provide the background on the validity and limitations of the measurements. At least one of the coauthors of this manuscript is also coauthor of such works:

Toohey et al. (2013) https://doi.org/10.1002/jgrd.50874 Hegglin and Tegtmeier (2017) The SPARC Data Initiative: Assessment of stratospheric trace gas and aerosol climatologies from satellite limb sounders. SPARC Report No. 8, WCRP-05/2017.

Author Response (A.2.1)

We agree with the reviewer and have revised the introduction to be more thorough in the background work. However, not every work recommended by the reviewer are mentioned. To include all of them, the discussion may become too diffusive. The introduction has been updated in order to provide better context for our case study and ensure the reader has a broader picture of the background and field. This includes edits to the text that incorporate some of the suggested references, as well as, several additional references that we feel helped to contextualize the discussion. These changes have significantly improved the introduction and help to set up the overall goal of the paper.

Related to the Introduction: the manuscript has two parts, the validation of the instrument and the case study. Therefore, I think that all the information relevant for the case study that lets to interpret the results should be presented first, included in section 1.

In this vein, the current section 6 should be moved earlier in the manuscript, before beginning the analysis and interpretation of the results. Also, the current figure 1 is right; still, I think that it would be good to include a similar isobaric synoptic map (to check the meteorological situation) and the corresponding map for the first lapse rate tropopause. Doing it would let the reader have a broad picture of the situation. Double tropopauses can happen because of several different conditions, and a priori all of them should be had into account. To do it, all this information is relevant. After it, I suggest to include a brief sentence discussing how the region chosen for the ER-2 flight is one of the central global areas of occurrence of double tropopauses including summer as Añel et al. (2008) shows (https://doi.org/10.1029/2007JD009697). The other work cited in the text and typical about the study of double tropopauses, Randel et al. (2007) do not show them for July over the region studied in this work.

Author Response (A.2.2)

We have made structural changes to the paper and further clarified that the objective of the case study is to identify the process of transport revealed by the observation and that the observation further demonstrate the scientific significance of the new measurement capability.

Specific changes:

1) Firstly, we have included a new figure showing 3 - 48-hour time steps (each day at 20:00 UTC) of PV on the 380 K surface for the 6 days leading up to the date of the case study (this is now Figure 2 in the paper). The Figure clearly shows a Rossby wave-breaking event has occurred in the days preceding the flight that results in mixing along the subtropical jet.

2) We have added a new figure (Figure 3) shows the PV on the 380 K (Figure 3 (a)) and 400 K (Figure 3 (b)) surfaces for the 07/21/2017 18:00 UTC time step. In the Figures, the tropospheric and stratospheric air masses are separated by the 6PVU contour on the 380 K surface and 8 pvu on the 400 K surface. Here it is observed that the mixing associated with the Rossby wave breaking results in a long low PV “tongue” consistent with tropospheric air that extends from the Western Pacific and tracks the subtropical jet across North America.

3) To characterize the vertical structure we have included a Figure (now Figure 4) that shows the height of the thermal tropopause and the location/extent and height of the secondary tropopause for the 07/21/2017 18:00 UTC time step. In these figures one can clearly see that there are several double tropopause regions located on the poleward of the subtropical jet. The SHOW measurements track crosses one of these regions. While additional time steps are not shown, it is useful to point out that the regions of double tropopause vary in extent from time-step to time-step. In fact, the double tropopause region that SHOW crosses becomes larger near the 21:00 UTC time step. A paragraph has been included in the text that discusses this Figure. We believe that the updated analysis provides the relevant context for the case study and justifies the suggestion that the moist filament observed along the second tropopause in Figure 6 (a) is likely of tropospheric origin.

4) The goal here is not to validate the SHOW measurements using the reanalysis data but rather show that the measurements are consistent with a mixing event. Therefore, the current section 6 has been removed and the discussion of the spatial extent of the event is now examined in Section 3 with the new Figures showing the full synoptic picture.

In Figure 2, I had to realise that the values of the horizontal axis are different for each subplot. Right now, it is harder to visualise the latitudinal variation and the assessment of the vertical 'peaks', but it is necessary to be able to compare all of them adequately. Therefore, please, use the same axis for every subplot. Also, it would be helpful to contextualise the air masses if you can add a horizontal line at the level of the thermal tropopause (first and second, if possible). In the caption, you have missed the degree symbol before the cardinal points.

Author Response (A.2.3)

The axes have been adjusted to be the same and we have included horizontal lines noting the altitudes of the first and second tropopause. The degree symbol has been added before the cardinal points in the caption as well as throughout the manuscript where it was missed.

Regarding Figure 3, I have several concerns that should be clarified and better discussed:

First of all, it would be useful in you can include the longitude value in the caption. Secondly, the authors do not say how they have computed the thermal tropopause. Did they use its definition (WMO, 1957)?. Was it retrieved from reanalysis?. It has to be clarified. Also, the use of model levels for the reanalysis could have improved the discussion. If you can use them, it would be better.

Author Response (A.2.4)

1. The longitude stayed nearly constant during the flight as mentioned in the text describing Figure 3 and in Section 2. We have added the following line to the caption of the figure: "The longitude is along the 124.5° W line and is nearly constant for the measurements."
2. There is no tropopause product in the ERA-5 reanalysis available to this work. The tropopause we used is derived from the 37 level temperature product. We stated this in the revision and have included a detailed description:

   "Here the tropopause is derived using the ERA-5 temperature field using the lapse rate definition (WMO, 1957; 1992) with a modification. The modified version locates the first tropopause as the lowest level where the lapse rate drops below 2 K/km and remains below that value on average for 1 km (instead of 2 km). A second tropopause is identified if the lapse rate increases above 2K/ km (instead of 3 K/km) and then decreases again below 2 K/km. This is done to remedy the coarse vertical resolution of the of the temperature data. This type of modification has been recognized to allow identification of the double tropopause derived from coarse resolution temperature data that is more consistent with high resolution observational data (Randel et al., 2007). In particular, our goal here is to highlight the spatial extent of the layered static stability structure as discussed in Sections 4-5."

About the plots: in Fig. 3a the isentropic entrainment in the lowermost stratosphere reaches 40.5 degrees N. However, in this region, the PV values are large (up to 6 PVUs, at least 5 PVUs). No doubt, the WV is of tropospheric origin, but such PV values are much higher than acceptable for tropospheric air. At these latitudes, the larger values expected for tropospheric air are 3.5-4 PVUs. If you check your Fig. 4a it seems clear that the 6 PVUs value that you mention in the text as a value for the tropospheric air, is seen in AURA, not so much in the SHOW measurements (and the AURA measurement fits better with the shape of the potential temperature lapse rate in Fig. 3b). Wang and Polvani (2011) (https://doi.org/10.1029/2010JD015118) and Añel et al. (2012) (http://dx.doi.org/10.1100/2012/191028) have already shown with idealized experiments and lagrangian models how the equatorward movement of air masses trough tropopause breaks at midlatitudes is also very important (and indeed they did it for regions close to the one studied here). Checking the Figure 4b, it could be argued that there is a fingerprint of the movement of stratospheric air equatorward through the break, because of the higher values of ozone that reach the 4 PVUs (near to the more accepted tropopause value) and 36.5 degrees N. Therefore, I think that you need to write the paragraphs from line 204-216 with a more complete discussion and better balance.

Author Response (A.2.5)

1) The PV value for representing the tropopause is the topic of Kunz et al., 2011. There the gradient based analysis showed that at 380K the average PV for identifying tropospheric to stratospheric change is 6 pvu. Although not shown it is around 8 pvu at 400K . We include this reference in the revision. We also emphasized in the discussion not the specific PV contour but the weakening of the PV gradient in the region indicates the tropopause break.

2) Yes the discussion focused on the poleward RWB as indicated in the new figures 2-4. For the purpose of this study, the resulting vertical layered structure above the subtropical break is the key. Equator-ward transport is also important but not the focus of this study.

A right way of checking the reality of the movement would be with using a lagrangian transport model (as in Añel et al. 2012). If you can include it, it would be a great addition to the manuscript, but I realise that it is not the goal of this work, so I do not consider it a 'must' here. But given that you do not provide it and on the ground of the tasks that I mention above, along with the text, you should relax the language and the level of the statement about poleward isentropic mixing. For example, in line 197, where you say 'it is widely accepted' because there are many different synoptic situations.

Author Response (A.2.6)

Indeed we focus the analysis on providing the high resolution measurement and evidence of the transport impact on lowermost stratospheric water vapor and the highlight of new measurement capability. This is clarified in the opening and abstract.

Finally, the summary and conclusion' section is short. I would include some discussion on the error of SHOW and how it could have impacted the results here presented. Also, I would find it interesting to include a reflection on the limitations of SHOW to sample similar episodes in more poleward latitudes. Given that SHOW seems to have a restriction below 13.5 km and that poleward the tropopause height decreases, is SHOW limited to sample these episodes only around the subtropical jet?. In line 304, the terminology of 'tropospheric intrusions' is used again. As said before, I think that talking about 'tropopause breaks' is correct in the context of this work.

Author Response (A.2.7)

We have updated Section 6 to be an expanded discussion and conclusion section. This section provides discussion on the limitations of the SHOW measurements and how these limitations may have impacted the study is now included in the paper. Specifically, we discuss the choice of the lower altitude cutoff. The lowest altitude cutoff of the measurements is primarily associated the optical depth. At some point, when the optical depth is below 1, scattered light from below is fully absorbed by the atmosphere. This generally occurs a few 3-5 km below the tropopause and varies from profile to profile. Algorithms are in development to actively determine this cutoff during the retrieval process. However, we did not have apriori knowledge of the meteorological picture prior to performing the retrievals. For the current study we chose 13.5 km to fix the altitude at a reasonable height (several km below the expected 15 km -18 km tropopause height for latitudes below the break) that we knew would provide accurate retrievals across the latitude range.

We also reiterate in the discussion section that we are not trying to validate the SHOW measurements with MLS and the reanalysis data. The SHOW measurements provide a much higher spatial sampling compared to either MLS or ERA5 and we are confident in the quoted uncertainties of the SHOW measurements. Therefore, the variability observed in the two-dimensional water vapour distribution

observed by SHOW is representative of the true state of the atmosphere. The reanalysis data provides the appropriate meteorological context and the MLS measurements serve to geophysical consistency with the SHOW measurements.

Minor corrections (A.2.8)

References: - The list of references is in the incorrect order. - Randel et al. 2007a and 2007b are not distinguished in the list of references.

- Only Randel et al., 2007a is referenced the paper now

Line 28 - de Forster and Shine Line 30 - Gettelman and Sobel, 2000 Line 44 - Appenzeller and Davies, 1992 Line 52 - Pan et al. 2010 is not listed among the references

- Gettelman and Sobel, 2000 Line 44 - Appenzeller and Davies, 1992 Line 52 - Pan et al. 2010 are no longer referenced in the manuscript
- de Forster and Shine, 1999 and 2000 are included

Table1-unitsofspeed–km/h(notkm/hr)

- Corrected

Line112-the international units of pressure are hPa, not mb

- Corrected

Line 133 - coarser

- Corrected

Line 168 - there is not an orange line in the figure

- Corrected

Lines 176-178 - this sentence is redundant. It has been discussed earlier in the text. I suggest removing it.

- Corrected

Lines 187-189 - in line 188 when you refer to the tropopause, it is hard to know if you refer to the first or the second; please clarify it. Also, it would be useful in you can include in the plot something (an 'A' and a 'B,' a star and a square,...) to make clearer to what region you refer.

- The text has been edited to be less ambiguous

Lines 248-251: the last sentence is obvious and can undermine the achievements of the SHOW instrument. I recommend to move it to the conclusions as a final reflection.

- This statement has been moved to the new discussion section (Section 6)

Line 269 - 20 degrees Figure 5 - caption - I would say ’230 and 235.5’. I read the plots from top to bottom and the one on the top corresponds to 230. As it is now, it can be not very clear.

- Corrected

Observational evidence of moistening the lowermost stratosphere via isentropic mixing across the subtropical jet

Jeffery Langille[1], Adam Bourassa[1], Laura L. Pan[2], Daniel Letros[1], Brian Solheim[1], Doug Degenstein[1], Daniel Zawada[1]

[1]Institute of Space and Atmospheric Studies, University of Saskatchewan, Saskatoon, S7N 5E2, Canada
[2]National Center for Atmospheric Research, Boulder Colorado, 3090 Center Green Drive, CO 80301, USA

Correspondence to: Jeffery Langille (jeff.langille@usask.ca)

Abstract. Isentropic mixing across and above the subtropical jet ~~in the presence of a double tropopause may be~~is a significant mechanism for stratosphere-troposphere exchange. In this work, we show new observational evidence on the role of this process in moistening the lowermost stratosphere. ~~We present an analysis of high spatial resolution two-dimensional measurements of the water vapour distribution that were~~The new measurement, obtained ~~using~~from the Spatial Heterodyne Observations of Water (SHOW) instrument during a demonstration flight ~~from~~on the NASA's ER-2 high ~~-~~altitude ~~ER-2 airplane. We focus on a set of measurements from 37° to 44° North, obtained on July 21, 2017 during a flight off the West coast of North America, where the instrument sampled the region above and~~ research aircraft, captured an event of poleward ~~of the subtropical jet.~~water vapour transport, including a fine scale (vertically ~ < 1 km) moist filament above the local tropopause in a high spatial resolution two-dimensional cross-section of the water vapour distribution. Analysis of these measurements combined with ERA5 reanalysis data reveals that this poleward mixing of ~~moist filaments~~air with enhanced water vapour occurred in the region of a double tropopause~~.~~ following a large Rossby wave breaking event. These ~~moist filaments are examined in the context of the meteorological fields in the ECMWF (ERA-interim) model output. It is shown that the observed moist filaments are consistent with isentropic mixing across and above the sub-tropical jet. These new~~ new observations ~~provide further evidence that the tropospheric intrusion associated with the double tropopause contributes to moistening of~~ highlight the importance of high resolution measurements in resolving processes that are important to the lowermost stratosphere water vapour budget.

1. Introduction

The distribution of water vapour in the upper troposphere and lower stratosphere (UTLS) region plays a critical role in the physical processes that couple the region to Earth's climate. This is especially true near the tropopause and in the lower stratosphere where the radiative sensitivity and climate impact of water vapour is ~~the most significant [Solomon et al., 2010]. In this region, mixing between tropospheric and stratospheric air masses results in spatial and temporal variability in the lower stratosphere that is not resolved in current climate models.~~ most significant (de Forster and shine, 1999; de Forster and Shine, 2002; Solomon et al., 2010). Several studies have shown that trends in stratospheric water vapour

affect long term and recent climate trends (e.g., Solomon et al., 2010; Dessler et al., 2013; Banerjee et al., 2019). Due to the strong gradient in the water vapour distribution across the tropopause and the fact that controlling mechanisms often involve small scale processes, quantifying stratospheric water vapour and its trends remains challenging for both observations and modelling (Kley et al., 2000; Gettelman et al., 2010; Riese et al., 2012; Högberg, et al., 2019; Nedoluha et al., 2017).

~~Several studies have suggested that this variability provides a mechanism for significant radiative forcing (or feedback) that has the potential to affect long term, as well as, recent climate trends [de Forster and shine, 1999; de Forster and Shine, 2002; Solomon et al., 2010]. Therefore, a detailed understanding of these processes is required in order to fully understand the impact of anthropogenic forcing of the climate [Stohl et al., 2003; Gettelman et al., 2000; Solomon et al., 2010].~~

~~The primary pathways for the flux of air mass into the stratosphere are well known [Holton, 1995; Dessler et al., 1999]. The simple picture described in Dessler et al., 1999 is followed here. In the tropics, deep convection on the ascending branch of the Brewer-Dobson circulation [Brewer, 1949; Dobson, 1956] pushes tropospheric air across the tropical tropopause layer (TTL). This air mass slowly ascends into the uppermost stratosphere or overworld (above the 380 K surface) where the isentropic surfaces lie in the stratosphere at all latitudes. During this process, moist tropospheric air is dehydrated as it passes through the cold point in the TTL. Over the course of weeks and months, this dry air is transported to the extratropical lower stratosphere as part of the descending branch of the circulation. The dehydration process in combination with methane oxidation accounts for the low water vapour mixing ratios that are observed in the stratosphere.~~

~~In the middle-world, isentropes intersect the tropopause and the tropical upper troposphere and the extratropical lower stratosphere air masses are coupled by isentropic mixing. This region is usually taken to lie between 310 K to 380 K where the layer poleward of the tropopause is referred to as the lowermost stratosphere (Holton et al., 1995). This mixing process is expected to involve finer scale processes and to show filamentary structures (Holton et al., 1995, Appenzeller et al., 1992). Chemical structures of quasi-isentropic mixing have been observed in the vicinity of the subtropical jet in association with Rossby wave breaking events [e.g., Pan et al., 2009; Ungermann et al., 2013].~~

~~Stratospheric intrusions during tropospheric fold events result in high stability air pushing deep into the troposphere and subsequently high ozone air (and low water vapour mixing ratios) below the tropopause [Stohl et al., 2003]. On the other hand, during tropospheric intrusions, unstable and moist tropospheric air enters the lower stratosphere. This typically coincides with the formation of a double tropopause above and poleward of the subtropical jet [Pan et al., 2009; Randel et al., 2007a; Randel et al., 2007b; Pan et al., 2010]. In both cases, filamentary structures are observed in chemical species that closely align with these isentropic surfaces. Filamentary structures have also been observed that do not align with these surfaces. Important questions remain regarding the small scale physical mechanisms that control these processes, as well as, which mechanisms dominate moistening of the lower stratosphere.~~

~~Current and historical satellite measurements lack the vertical resolution that is required to constrain water vapor processes in the UTLS [Randel and Jensen, 2013] , and merging of individual short term records is challenging, partly due to the limited sampling [Hegglin et al., 2014]. These measurements cannot explain observed variability in lower stratospheric water vapour. Understanding the variability and long term changes in UTLS water vapor at the level required to resolve differences in reanalysis models requires global, high-resolution observations [Randel and Jensen, 2013].~~

~~Resolving the spatial structures in the vertical distribution of water vapour requires a vertical resolution of less than several hundred meters and an along track sampling capability on the order of 10 km. Currently, one of the best measurements of this type are performed using the Microwave Limb Sounder (MLS) on the AURA satellite, which provides 2 km – 5 km vertical resolution in the UTLS with profiles retrieved every ~165 km in latitude [Birner et al., 2006; Müller et al., 2016].~~

In this work, we present a case study of high-spatial-resolution observations of UTLS water vapour that has been enabled by new measurement technology. The measurements, using the Spatial Heterodyne Observations of Water (SHOW) instrument on board the NASA ER-2 research aircraft during a demonstration flight, captured an event of water vapour transport into the lowermost stratosphere across the subtropical jet. Using ECMWF ERA-5 reanalysis product, we demonstrate the transport is driven by a large scale Rossby-wave breaking event and in association with the occurrence of a double tropopause. Together, the result demonstrates the importance of isentropic transport processes for the stratospheric water vapour budget, and the importance of high-resolution water vapour measurements in the UTLS.

In the middle-world, the layer of atmosphere between 310 K and 380-400 K, the isentropic surfaces intersect the tropopause in the subtropics (Holton, 1995 and reference therein). A ubiquitous feature here is a sudden drop in the thermal tropopause near the subtropical jet, known as the "tropopause break". The layer poleward of the break is defined as the lowermost stratosphere and is strongly influenced by transport via isentropic mixing associated with Rossby wave breaking (e.g., Chen, 1995; Scott and Cammas, 2002). The role of isentropic mixing in the budget of lowermost stratosphere water vapour has been highlighted by both in-situ airborne and balloon observations (e.g., Dessler et al., 1995; Hintsa et al., 1998; Ray et al., 1999) and satellite measurements (e.g., Pan et al., 1997). A number of more recent studies have shown that the occurrence of a double tropopause is associated with Rossby-wave breaking and large-scale poleward transport. Chemical signatures of this type of transport has been observed in ozone and a number of other species (Pan et al., 2009; Homeyer et al. 2011; Ungermann et al., 2013). The observation reported in this work, however, represents the first such measurement of the 2-dimensional structure of the water vapour distribution.

The Spatial Heterodyne Observations of Water (SHOW) instrument is a new limb sounding satellite prototype originally designed and built at York university that is being further developed in collaboration between the University of Saskatchewan and the Canadian Space Agency to provide high vertical resolution (< 250 m) measurements of water vapour with high precision (< ±1 ppm) in the UTLS region. The instrument implements a limb imaging spatial heterodyne spectrometer (SHS) to obtain vertically resolved images of the water vapour spectrum using limb-scattered sunlight in a 2 nm

spectral window centered on 1364.5 nm (Langille et al., 2017). Each SHOW measurement is inverted using the optimal estimation approach to obtain the vertical water vapour profile for each along-track sample (Langille et al., 2018).

The SHOW prototype flew several demonstration flights on NASA's ER-2 ~~aircraft~~airplane in July, 2017 in order to validate the measurement approach and to demonstrate the along-track sampling capabilities of the instrument. The SHOW measurement technique, retrieval approach and instrument performance was validated during an Engineering flight that was performed on July 17, 2018 (Langille et al., 2019). Comparison with co-located radiosonde measurements were found to be in excellent agreement, with differences of < 1 ppm above 15 km (near the thermal tropopause) and < 2-5 ppm below 15 km, due to both natural variability between the observations and measurement precision.

~~In~~ The analysis of this ~~paper, we present observations of the two dimensional distribution of UTLS water vapour obtained during a~~work focuses on another flight ~~on board the ER-2~~performed on July 21, 2017. The flight path ~~was chosen to provide sampling~~(Figure 1), across several degrees of latitude off the west coast of North America from roughly 34° North to 48° North along the ~~–124.5°West longitude line. We focus our analysis on a one hour window of measurements where SHOW sampled the water vapour distribution near the subtropical jet.~~ –124.5° West longitude line, was chosen in an attempt to observe potential mixing near the tropopause break in a region known to have a relatively frequent occurrence of double tropopauses in summer season [Anel et al., 2008]. This mixing process often produce fine scale filaments that are difficult for the satellite measurements and the large-scale models to resolve. The result of the measurement indeed shows fine scale water vapour structures which reveals poleward mixing of moist filaments in the region of a double tropopause, demonstrating the capability of the new measurement technology in capturing the climate relevant water vapour transport process.

Meteorological fields determined from the ECMWF ERA-5 reanalysis are used to examine the dynamical setting of the measurements. To support the process understanding, the Rossby-wave breaking event that proceeds the observation is examined using isentropic maps of potential vorticity (PV). Also examined to support the process identification is the nearly coincident retrievals of ozone and water vapour from the AURA-MLS instrument.

2. The Spatial Heterodyne Observations of Water (SHOW) instrument

The SHOW instrument is spatial heterodyne spectrometer that has been optimized for limb viewing observations of limb-scattered sunlight within a vibrational band of water. The limb is imaged conjugate to the SHS interference fringes such that each interferogram row and subsequently each spectral row in the image is mapped one-to-one to line of sight at the limb. Each sample provides a vertically resolved spectral image with ~0.03 nm spectral resolution in a 2 nm window centered on 1364.5 nm. These vertically resolved spectral images are inverted using a non-linear optimal estimation

approach to obtain the vertical distribution of water vapour. The SHOW measurement technique and retrieval algorithm is discussed in previous publications [Langille et al., 2018; Langille et al., 2019].

Instrument parameter	Specification
ER-2 airplane altitude	**~21.34 km (70000 ft max)**
Airplane speed	**~760 km/~~hr~~h (maximum at altitude)**
Field Of View	**4° vertical by 5.1° horizontal**
Temporal cadence	**1Hz or 0.5 Hz**
Spatial sampling at the surface	**~1 km @ 1 Hz**
Instantaneous angular vertical resolution	**0.0176 degrees**
Retrieval altitudes	**13 km to 18 km**
Retrieval grid	**250 m**
Mass	**222.68 lbs [101 kg]**
Power	**465 W (peak), 200 W (average)**
Dimensions	**(0.465 m × 1.32 m× 0.38 m)**
Spectral Resolution (unapodized)	**~0.03 nm**
Spectral range	**1363 nm – 1366 nm**

Table 1 SHOW ER-2 instrument parameters

The prototype SHOW instrument is optimized for observations from NASA's ER-2 airplane and is mounted in a forward looking wing pod to observe a 4 degree vertical by 5.1 degree horizontal field of view. Flying at an altitude of 21 km, the viewing geometry and optical configuration provides a vertical sampling at the limb tangent point of 51 m to 171 m, increasing towards the ground tangent. The instrument utilizes anamorphic optics to average over the scene in the horizontal dimension; therefore, no horizontal (longitudinal) scene information is obtained. Using this configuration, retrievals are performed on a 250 m retrieval grid with no smoothing to provide an approximate vertical resolution of 250 m from 13 km up to 18 km with precisions better than 1 ppm. The instrument can be operated using sampling rates from 0.1 Hz up to 2 Hz mode; however, the measurements discussed in this paper are obtained using a sampling rate of 1Hz. This provides an approximate raw along track sampling of ~~1~~0.5 km at the surface (or ~0.005 degrees latitude). The primary instrument specifications are listed in Table 1 and the full instrument configuration is presented in Langille et al., 2019.

3. ER-2 flight ~~path~~track and the metrological background

The measurements discussed in this paper were obtained during a flight on board the ER-2 performed on July 21, 2017 between 18:00 UTC and 19:00 UTC off the Western coast of North America. For analysis of the meteorological fields within this measurement window we utilize the ECMWF (ERA-~~interim) model output. The model data is~~5) reanalysis products, which are provided in 1-hour time steps on a 0.25 degree x 0.25 degree grid (latitude x longitude) at 37 pressure levels from 1 mbar up to 1000 mbar.

~~The~~ To provide the dynamical background of the flight track, the zonal wind at the 175 ~~-~~hPa level (approximately 13 km altitude) for the 18:00:00 UTC time step on July 21, 2017 is shown in Figure 1.

The zonal wind ~~plot~~field shows a double jet structure with the subtropical jet located near ~~45° degrees~~ 35° North ~~with a secondary branch located close~~ and the polar jet near ~~35° degrees~~ 45°North. Both features have jet cores (with winds > 40 m/s) that are located over the Pacific Ocean ~~and the~~ . As the subtropical jet is shifting north, downstream in an anticyclonic flow, the two jets ~~weaken as they approach the coast and become superimposed~~ merge over North America. This configuration is formed with a large-scale Rossby wave-breaking event that developed over several days prior to the SHOW measurements, and is demonstrated in Figure 2 using the 380 K isentropic potential vorticity in 48-hour intervals over a six days period. To further connect with the ER-2 track, the potential vorticity on the 380 K and 400 K surfaces is shown in Figure 3 for the 21/07/2017 time step. Here, the separation between stratospheric and tropospheric air occurs near 6 PVU and 8 PVU, respectively (Kunz et al., 2011), which is the noted by the white transition region between red (low PV air and tropospheric) and blue (high PV air and stratospheric) colors in the figures. A well-defined low PV structure consistent with tropospheric air is observed on the 380 K surface that extends from the Western Pacific up to the extratropical region over North America as a result of the wave breaking.

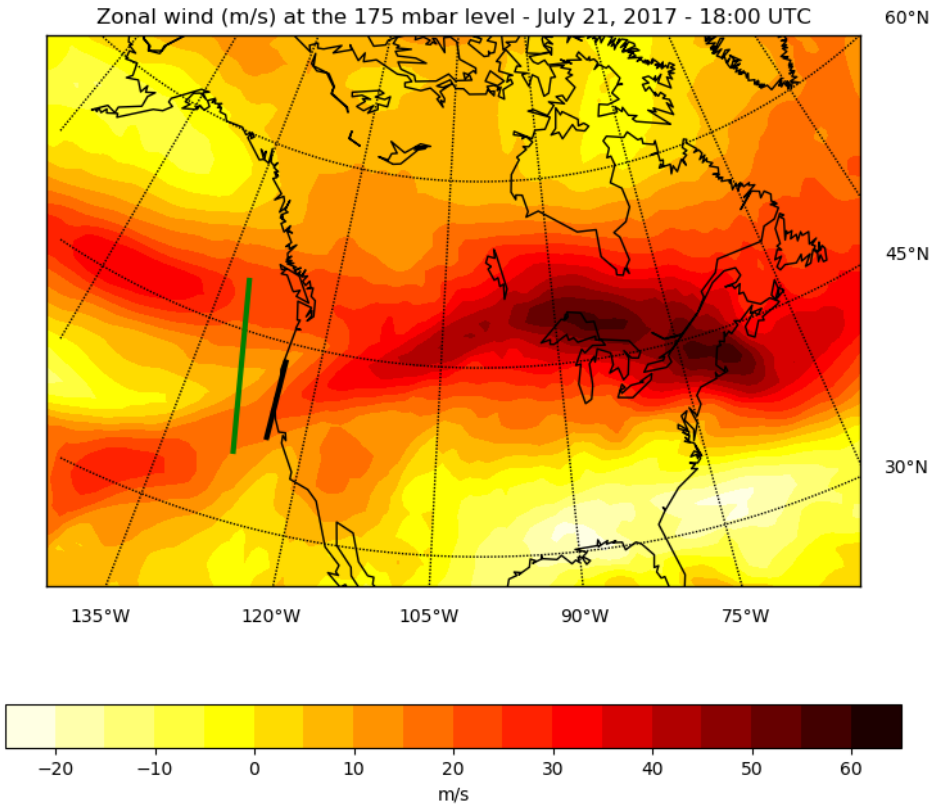

To characterize the dynamical structure vertically, the height of the thermal tropopause and the occurrence of the double tropopause is shown in Figure 4. Here the tropopause is derived using the ERA-5 temperature field using the lapse rate definition (WMO, 1957; 1992) with a modification. The modified version locates the first tropopause as the lowest level where the lapse rate drops below 2

K/km and remains below that value on average for 1 km (instead of 2 km). A second tropopause is identified if the lapse rate increases above 2K/ km (instead of 3 K/km) and then decreases again below 2 K/km. This is done to remedy the coarse vertical resolution of the of the temperature data. This type of modification has been recognized to allow identification of the double tropopause derived from coarse resolution temperature data that is more consistent with high resolution observational data (Randel et al., 2007). In particular, our goal here is to highlight the spatial extent of the layered static stability structure as discussed in Sections 4-5. The height distribution of the primary tropopause is shown in Figure 4 (a). The distribution of the secondary tropopause, shown in Figure 4 (b), is consistent with the formation mechanism of a poleward wave breaking along the subtropical jet (Pan et al., 2009). Although not shown here, the double tropopause features have varying strength from time-step to time-step on the days leading up to and after the flight. Occurrences of double tropopauses are common in this region with the highest occurrence rate in the winter [Swartz et al., 2014]; although, they are also observed in the summer season [Anel et al., 2008].

The ER-2 flight track with the SHOW instrument for the 18:00 UTC to 19:00 UTC time period, as indicated in Figures 1, 3 and 4, includes the edge of a large double tropopause region that extends off the Western coast of the United States. For process verification using an independent measurement, we identified a near co-located MLS satellite observation track, also marked on Figures 1, 3, and 4. Analysis of the SHOW and MLS measurements are discussed in Section 4 and Section 5 respectively.

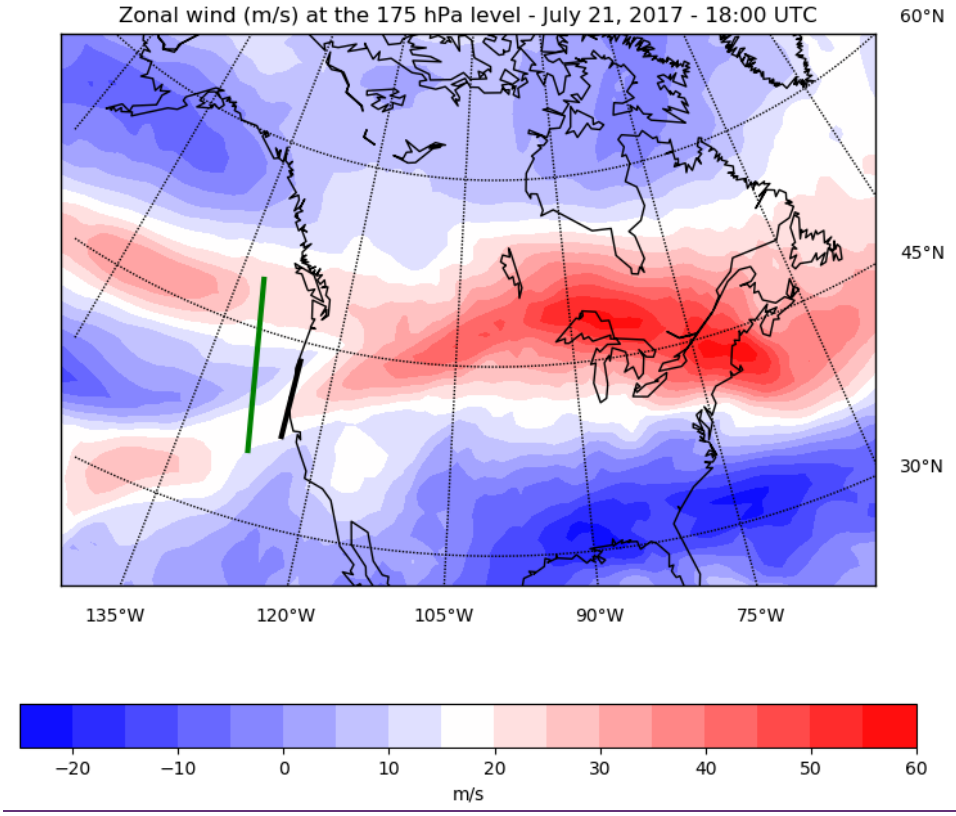

Figure 1 Zonal wind on the 175 hPa surface~~.~~ for the 18:00 UTC, July 21, 2019 time step. The ER-2 flight track with SHOW measurement ~~track~~ is shown as the ~~dark~~ black line and the closest measurement track of the AURA-MLS instrument is as the dark green.

~~The measurement track of the SHOW instrument for the 18:00 UTC to 19:00 UTC time period is shown as the thick black line in Figure 1. Along this track, SHOW obtained high vertical resolution (< 250 m) measurements of UTLS water vapour around the tropopause (13 km – 18 km). The sampled region begins near 37° N on the southern edge of the primary jet feature and ends on the southern edge of the secondary jet feature near 44° N. These measurements were then averaged by latitude to increase the signal to noise ratio, resulting in an along track sampling of approximately 0.32 degrees latitude (approximately 36 km at the ground).~~

~~For comparison, the thick green line in Figure 1 shows the measurement track of the AURA-MLS satellite instrument at approximately 21:51 UTC - roughly 2 hours after the SHOW measurements were performed. Along this track, the MLS instrument sampled the same geophysical feature along a slightly different path with an along track sampling of 300 km and a vertical resolution of 3-5 km in the UTLS. The MLS measurements have a courser spatial resolution and the sampling is not exactly coincident with SHOW. Therefore, some differences are expected between the measurements. However, both sensors sample nearly the same region in the vicinity of the subtropical jet. Therefore,~~

~~the MLS measurements are used to check for consistency with the meteorological picture in comparison with the SHOW measurements.~~

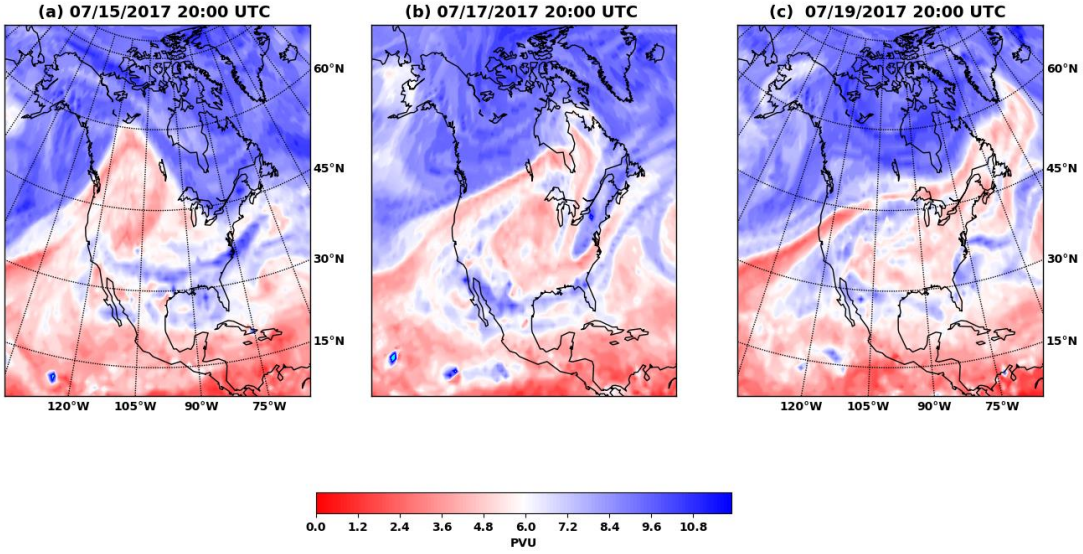

Figure 2 Potential vorticity on the 380 K isentropic surface on 07/15/2017, 07/17/2017 an 07/19/2017 showing a Rossby wave breaking event several days prior to the SHOW measurements.

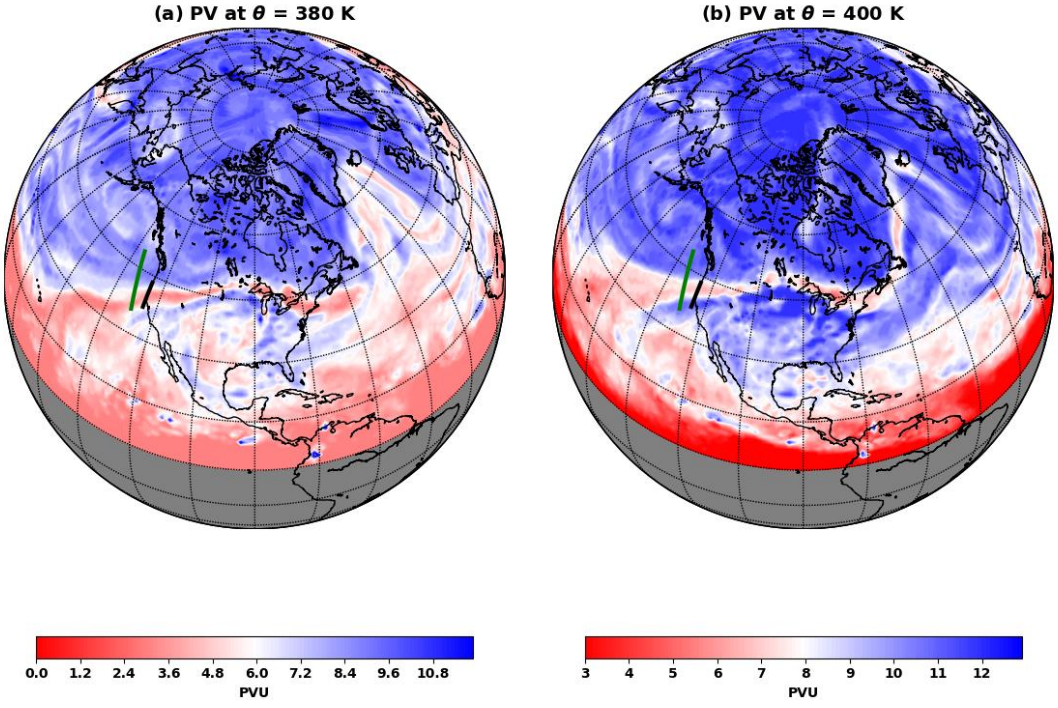

Figure 3 Potential vorticity on the 380 K (a) and 400 K (b) isentropic surfaces for the 18:00 UTC, July 21, 2019 time step. The measurement track of SHOW and MLS are shown in black and green respectively.

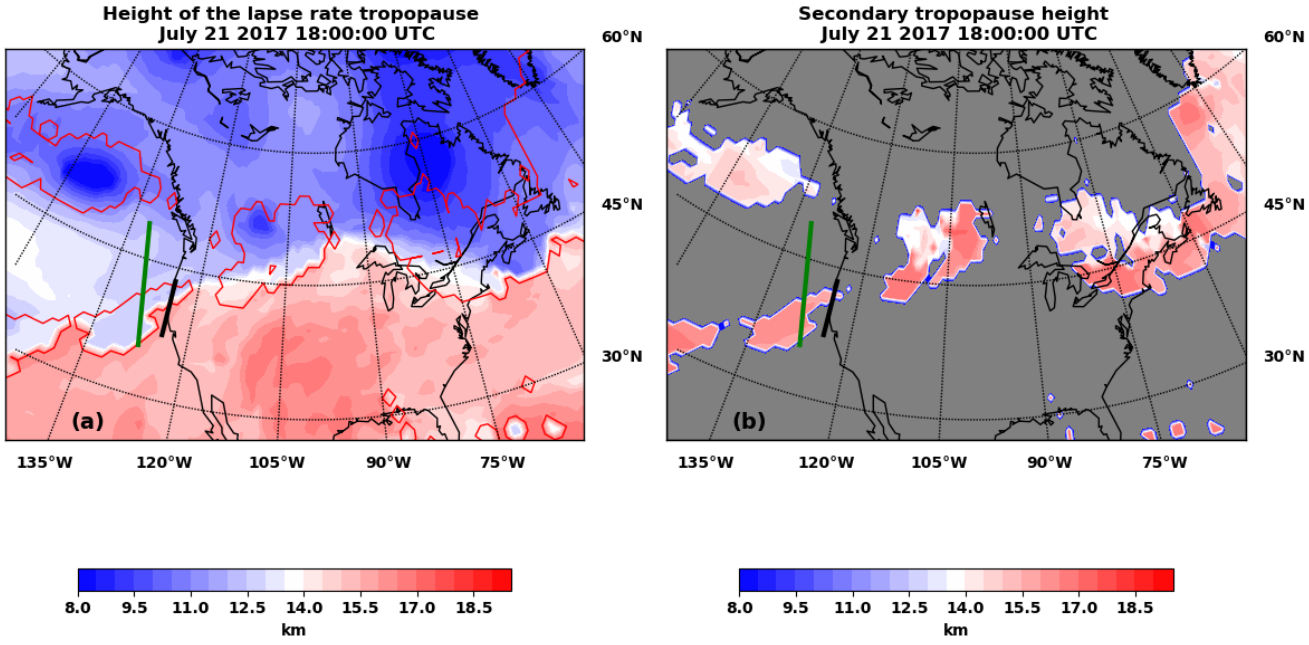

Figure 4 Height of the thermal tropopause (a) and the height of the secondary tropopause (b) for the 18:00 UTC time step. The red outline in (a) denotes the edge of the double tropopause regions shown in (b). The measurement track of SHOW and MLS are shown in black and green respectively.

4. SHOW Observations

~~Each of the SHOW limb images was processed to obtain a vertical profile for each sample obtained along the flight track shown in Figure 1. Three~~We begin the analysis of SHOW water vapour measurements with three example ~~SHOW water vapour~~ profiles ~~are~~, shown in Figure ~~2~~5 (a-c~~). The profiles~~), which correspond to the latitude bins centered at 37.4 degrees North profiles, 41.87 degrees North and 43.48 degrees North respectively. ~~-~~ Each example shows the set of 10 samples obtained within in each latitude bin (black) and the mean of the sample set (red). The observed variance in the water vapour distribution closely matches the 1-2 ppm measurement error predicted by propagating the noise through the retrieval. The red error bars show the precision for the averaged measurements which is less than < 0.3 ppm for most measurement altitudes. The upper and lower boundaries of the retrievals presented in this paper are 18 km and 13.5 km respectively. The altitude of the first and second lapse rate tropopause are shown as blue solid and dashed lines respectively.

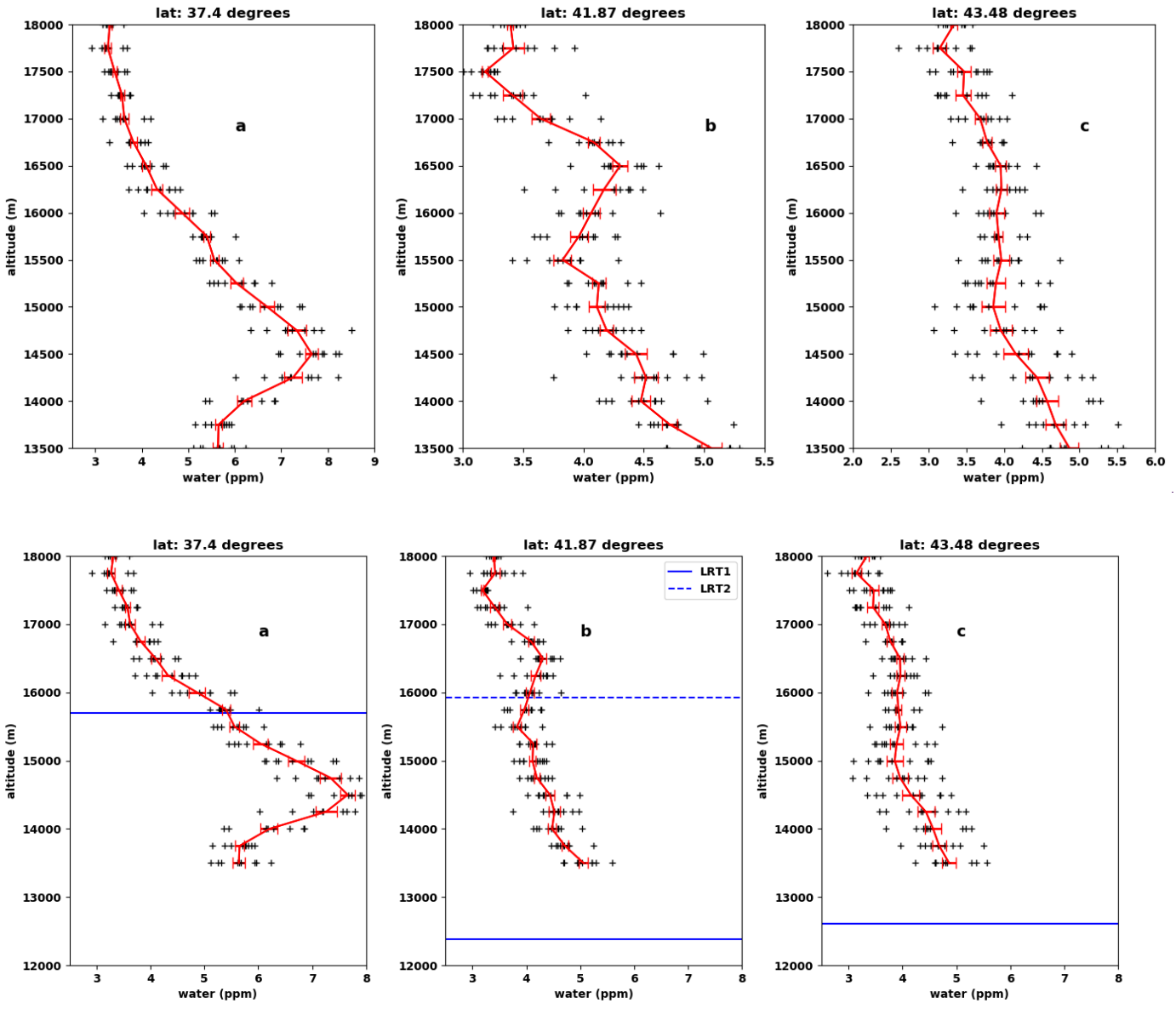

Figure 5 Example show profiles at 37.4° N (a), 41.87° N (b), and 43.48° N (c). All profiles lie closely along the -124.5 ~~degree~~° W in longitude ~~line~~. The black data points correspond to each of the individual profiles and the red line is ~~the line passing through~~ the average of all latitude measurements in each altitude bin. The error bars show the precision of the averaged measurements. The first and second tropopause are identified in the Figure with the solid blue and dotted blue lines respectively.

For the 37.4° N measurement, the water vapour mixing ratio increases to a maximum near 14.5 km and then decreases rapidly with increasing altitude. The water vapour mixing ratio is also found to decrease slightly below 14.6 km. In the current analysis, the lower boundary of the retrieval is at 13.5 km and therefore doesn't capture the expected increase of water vapour at altitudes below 13.5 km. At 41.87° N a secondary peak in the water vapour profile is observed near 16.5 km. The amount of water vapour

decreases slightly below this peak and then continues to steadily increase with decreasing altitude. Further along the flight track, at 43.48° N, the peak at 16.5 km has diminished and the amount of water vapour increases slowly with decreasing altitude.

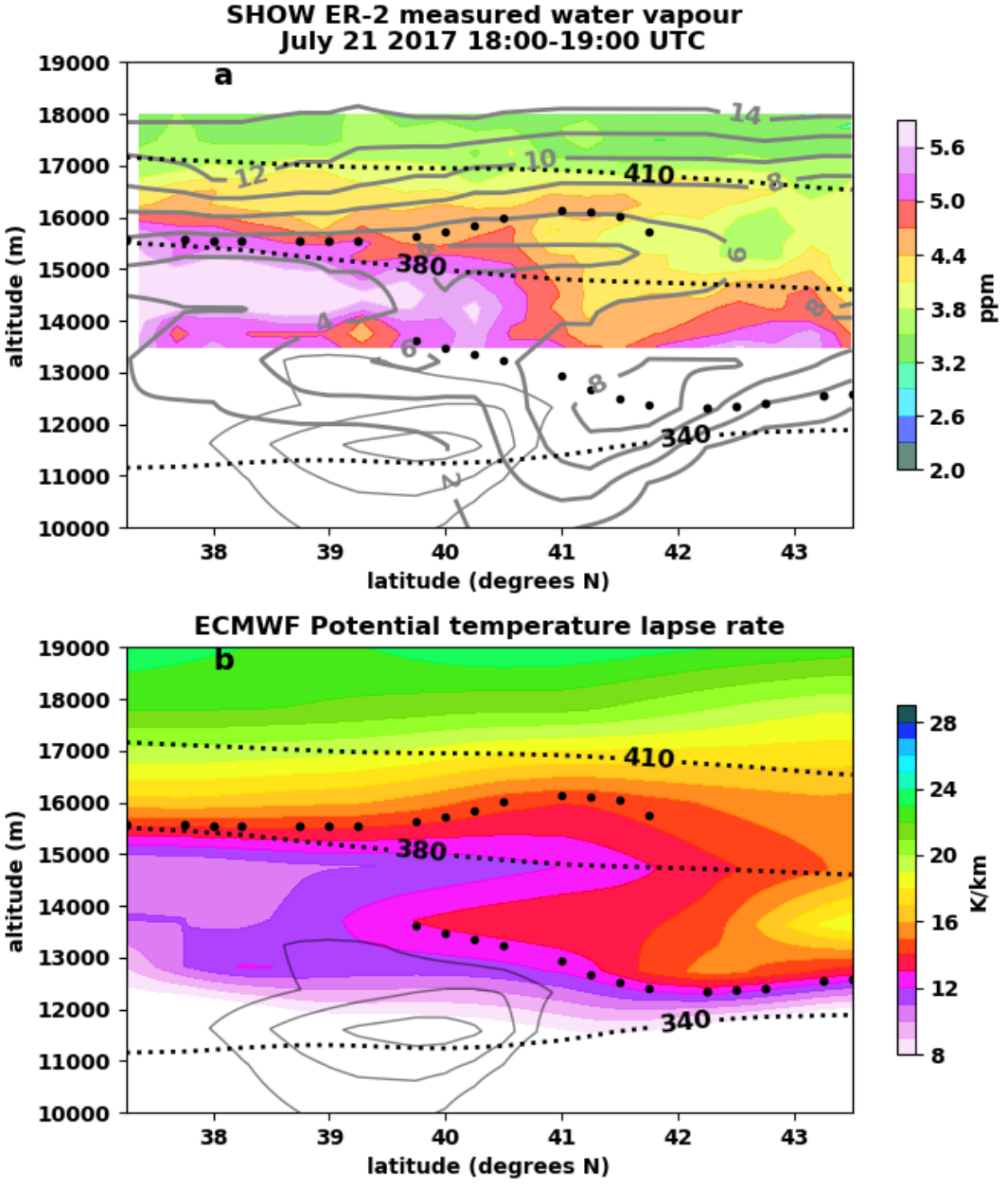

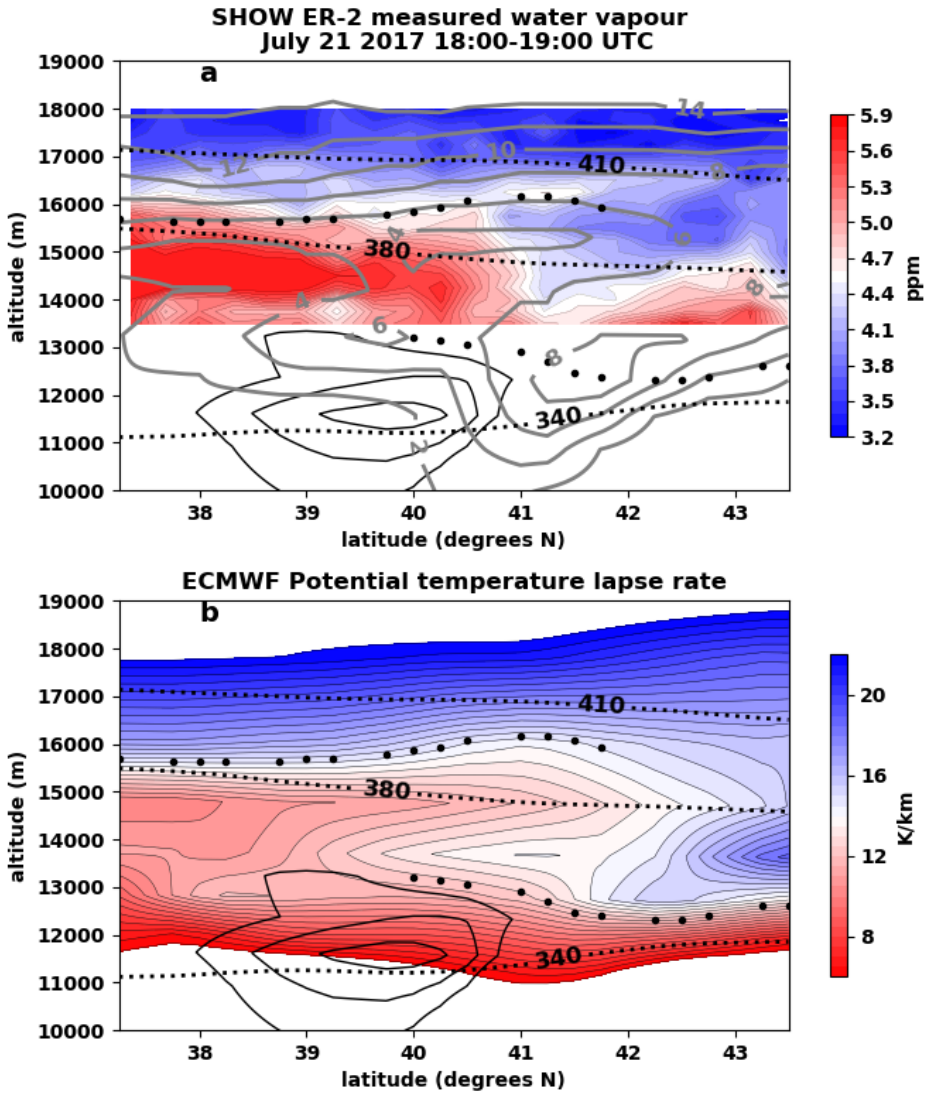

Figure 6 SHOW measured water vapour profile (from 18:00 UTC to 19:00 UTC) (a) and the potential temperature lapse rate determined from the ECMWF reanalysis for the 19:00 UTC time step along the SHOW measurement track (b). The dark dotted line shows the location of the thermal tropopause. The grey contours show the potential vorticity, several zonal wind contours are shown in light grey, and the light black dotted line shows the 340 K, 380 K and 410 K isentropes respectively. The longitude is along the 124.5° W line and is nearly constant for the measurements.

All of the measured water vapour profiles obtained along the flight track are stacked and plotted as a single data curtain in Figure ~~3~~6 (a). ~~The two dimensional profile that is~~ Along this track, SHOW obtained high vertical resolution (< 250 m) measurements of UTLS water vapour around the tropopause (13 km – 18 km). These measurements were then averaged by latitude to increase the signal to noise ratio, resulting in an along track sampling of approximately 0.32 degrees latitude (approximately 36 km at the ground). The result provides a high vertical resolution time (latitude) – height cross-section of the

water vapour distribution along the flight track. ~~To aid in the interpretation of the observed spatial variability we utilize the~~The dynamical fields, including zonal wind, potential temperature, potential vorticity and the derived tropopause locations from the ECMWF reanalysis (~~19~~18:00 UTC time step) ~~and plot several zonal wind (black) and potential vorticity (PV) (orange) contours~~are overlaid on top of the water vapour measurements. ~~The~~The dynamical structure in the cross-section co-located with the flight track is further examined in Figure 6 (b), where the structure of the static stability is highlighted using the potential temperature lapse rate determined from the reanalysis data ($PTLR = {\Delta\theta}/{\Delta z}$~~) is shown in Figure 3 (b) for the same region and time step.~~). In both figures, the 340 K, 380 K and 410 K isentropes are shown as the thin dotted lines and the thick black dots identify the location of the thermal tropopause.

~~The subtropical jet is in Figure 3 centered at the tight zonal wind contours (light grey) near 39.9 degrees at an altitude between 11-12 km. South of 39.9 degrees latitude, the thermal tropopause sits at an altitude of close to 15.5 km. Near 39.9 degrees we observe a break in the tropopause and record a double tropopause that extends from 39.9 degrees to 42 degrees. At the break, the primary tropopause drops to below 13.5 km and remains at this altitude or lower for higher latitudes. The tropopause break is a common feature of the thermal tropopause definition and is a ubiquitous feature found on the poleward side of the subtropical jets in observations [Randel et al, 2007 b], as well as, climate models [Manney, 2014].~~

~~From Figure 3, the~~The 410 K isentrope lies entirely in the stratosphere (in the overworld) at all latitudes. Above the 410 K isentrope, the water vapour mixing ratio is observed to have values between 3.0 ppm – ~~3.8~~4.0 ppm which defines the background water vapour mixing ratio in the lowermost stratosphere. Near the tropopause (in the middleworld), sharp spatial structures are resolved that have gradients on the order of 0.5 ppm per 250 m sampling bin. SHOW does not record the water vapour distribution below the 340 K isentrope since the retrieval cuts off at an altitude of 13.5 km. Discussion of this lower boundary is presented in Section 6.

~~Following from Figure 3 (a), SHOW recorded a large peak in the water vapour mixing ratio at roughly 14.6 km that extends from around 37° N to 40.5° N. The location of the thermal tropopause tracks the strongest gradients in the water vapour profile since the layer of air just above the tropopause acts as a strong barrier to vertical motions, resulting in a rapid decrease in water vapour above the tropopause. Correspondingly, a sudden drop in the amount of water vapour is recorded near 39.9° N coinciding with the tropopause break. After the break, the strongest gradient in the water vapour profile drops to nearly 13.5 km and continues to closely track the thermal tropopause.~~

~~Most interestingly, a well-defined moist filamentary structure is observed above and poleward of the tropopause break that coincides with the presence of a double tropopause. This structure has a water vapour mixing ratio that is larger than the background stratosphere by 1-1.8 ppm from 39.5° – 42°North within a 1 km region that is centered near ~16.5 km. The structure also roughly aligns with the isentropic surfaces.~~

~~It is widely accepted [Pan et al., 2009; Randel et al., 2007b; Gettelman et al., 2011] that the formation of the double tropopause on the poleward side of the subtropical jet is the result of the~~The dynamical structure of the cross-section identifies the flight track extended over a well-defined tropopause break over the jet core, which is indicated by tight zonal wind contours (black) near 39.9° latitude. South of 39.9° latitude, the thermal tropopause sits at an altitude of close to 15.5 km. The region of 39.9° to 42° has a double tropopause structure. More importantly, the region of the tropopause break has layered structure of static stability, showing a layer of low stability, tropospheric like air mass extending poleward over the primary tropopause. Consistent with the stability structure, the PV field (grey) in the region shows weakened gradient. Overall, the dynamical background has a large similarity with the observed tropospheric intrusion from the HIRDLES satellite ozone case study (Fig. 1 in Pan et al., 2009).

Water vapour measurements from SHOW (Figure 6 a) recorded a layer with water vapour mixing ratio greater than 5 ppmv which is much higher than the stratospheric background, centered at roughly 14.6 km, and extends poleward to about 40.5° above the local primary tropopause. Note that the layer in between the two tropopauses where the PV distribution shows a weakened gradient between the 4 and 8 pvu contours, indicating a weakened tropopause (Pan et al., 2009; Kunz et al., 2011a; 2011b). Further poleward, the SHOW measurements captured a part of layer with enhanced water vapour above the primary tropopause between 41.5°N and 43.5° N. The moist layer is also co-located with the weakened PV gradient.

While the static stability structure of the cross section (Fig 6b) indicates a case of intrusion of low static stability air from the subtropical troposphere into the mid-latitude lowermost stratosphere~~. Such intrusions result in isentropic mixing across and above the subtropical jet [Gettelman et al., 2011]; therefore, UTLS species, such as water vapour and ozone act as tracers of these events. The rough alignment of the isentropic surfaces with the moist filament recorded by SHOW suggests isentropic mixing between tropospheric air~~, the quasi-isentropic transport indicated by the SHOW water vapour cross-section is not entirely matching the stability structure. Considering that the observation is made in the advent of the Rossby wave breaking event, it is physically reasonable that the dynamical field and chemical structure are no longer intact, which is a sign of an irreversible transport. It is also likely due to the ERA5 products available to the analysis are given in much coarser vertical resolution compared to the SHOW measurements. The important point is that there is a clear process identification supported by both the water vapour measurement and the ~~lowermost stratosphere.~~

~~To support this interpretation we examine the PV and PTLR in the reanalysis data. Accordingly, the dark grey contours in Figure 3 (a) show the potential vorticity from 2 PVU to 14 PVU in 2 PVU increments. The surface defined by the 6 PV contour appears to characterize a dynamical surface that separates tropospheric and stratospheric air. Note that a patch of low PV air (< 4 PVU) is recorded near 15 km with a spatial range that extends from 39.5° – 42° N. The shape of the feature is strikingly similar in structure to the moist filament observed by SHOW at roughly 1.5 km higher altitude (~16.5 km).~~

~~The associated PTLR (shown in Figure 3 (b)) also tracks the overall spatial structure that is observed in the water vapour distribution. This is anticipated since the PTLR provides a measure~~dynamical field analysis. We will see a similar shift in the analysis of the ~~static stability of the air. Therefore, sharp gradients are expected to mark the separation between low stability tropospheric air and high stability stratospheric air. Along the SHOW measurement track, tropospheric air is primarily characterized with a PTLR < 12 K/km and stratospheric air is characterized with a PTLR > 12 K/km. A filamentary structure with PTLR < 12 K/km is observed to extend from 39.5° – 42° near ~15 km. This structure of low static stability air coincides with the presence of the double tropopause and matches a similar feature that is evident in the potential vorticity, as well as, the moist filamentary structure observed by SHOW at an altitude of ~16.5 km.~~

~~The offset in altitude between the filamentary structure observed by SHOW and the spatial structure that is observed in the PV and PTLR fields could be due to several reasons. For example, the SHOW instrument is a limb viewing instrument; therefore, this may be a consequence of the limb viewing geometry. In addition, the meteorological data is determined from a model and it is entirely possible that the model does not fully capture the true geophysical state of the atmosphere. We will see through a comparison with the~~ MLS ~~measurements of~~ water vapour and ozone ~~that a similar shift is also observed in that dataset. Therefore, it is most likely that the reanalysis does fully represent the finer scale structure during this event.~~ data in the following section.

5. AURA MLS ozone and water vapour

~~The AURA-MLS~~ For process verification, we examine measurements of water ~~vapor~~vapour and ozone that were obtained along a nearly coincident measurement track ~~are~~as shown in Figure ~~4 (~~1 (solid green line). The AURA-MLS satellite instrument obtained measurements along this track at approximately 21:51 UTC - roughly 2 hours after the SHOW measurements were performed. Along this track, the MLS instrument sampled the same geophysical feature along a~~)~~ slightly different path with an along track sampling of 168 - 230 km and a vertical resolution of 1.3-3.2 km in the UTLS (316 hPa - 46 hPa). The MLS measurements have a coarser spatial resolution and the sampling is not exactly coincident with SHOW. Therefore, some differences are expected between the measurements. However, both sensors sample nearly the same region in the vicinity of the subtropical jet. Therefore, the MLS measurements are used to check for consistency with the meteorological picture in comparison with the SHOW measurements.

~~Figure 4~~

The AURA-MLS measurements of water vapour and ozone are shown in Figure 7 (a) and Figure 7 (b) respectively. The corresponding PTLR plot is shown in Figure ~~4~~7 (c). For this comparison we use the 22:00 UTC time step of the ECMWF ERA5 reanalysis since it is the closest available time step to the MLS measurements which occurred at close to 21:50 UTC.

The distributions of the two trace species have a spatial structure that matches the general shape of the structure observed in the PTLR plot and PV contours. As expected, the vertical distributions of the trace

species are basically inverted, with water vapour decreasing with increasing altitude and vice versa for ozone. Most importantly, a filamentary structure is observed that extends from 36 N to 42 N near 16 km and coincides with the presence of a double tropopause. Again, the feature matches a similar structure that is observed in the corresponding PTLR plot and PV contours at a lower altitude (~ 15 km).

Taking the sharpest gradient in the PTLR to define the boundary between tropospheric and stratospheric air we see that tropospheric air is primarily characterized with a PTLR < 12 K/km and stratospheric air is characterized with a PTLR > 12 K/km. Therefore, as was the case with the SHOW measurements, the observed filamentary structure with PTLR < 12 K/km is consistent with the intrusion of a low static stability air from the subtropical troposphere into the mid-latitude lower stratosphere. ~~This~~Mixing on the poleward side of the subtropical jet results in ~~the formation of the double tropopause~~moistening and ~~the transport of moist tropospheric air and~~diminished ozone ~~depleted air into the mid-latitude lower~~in the lowermost stratosphere.

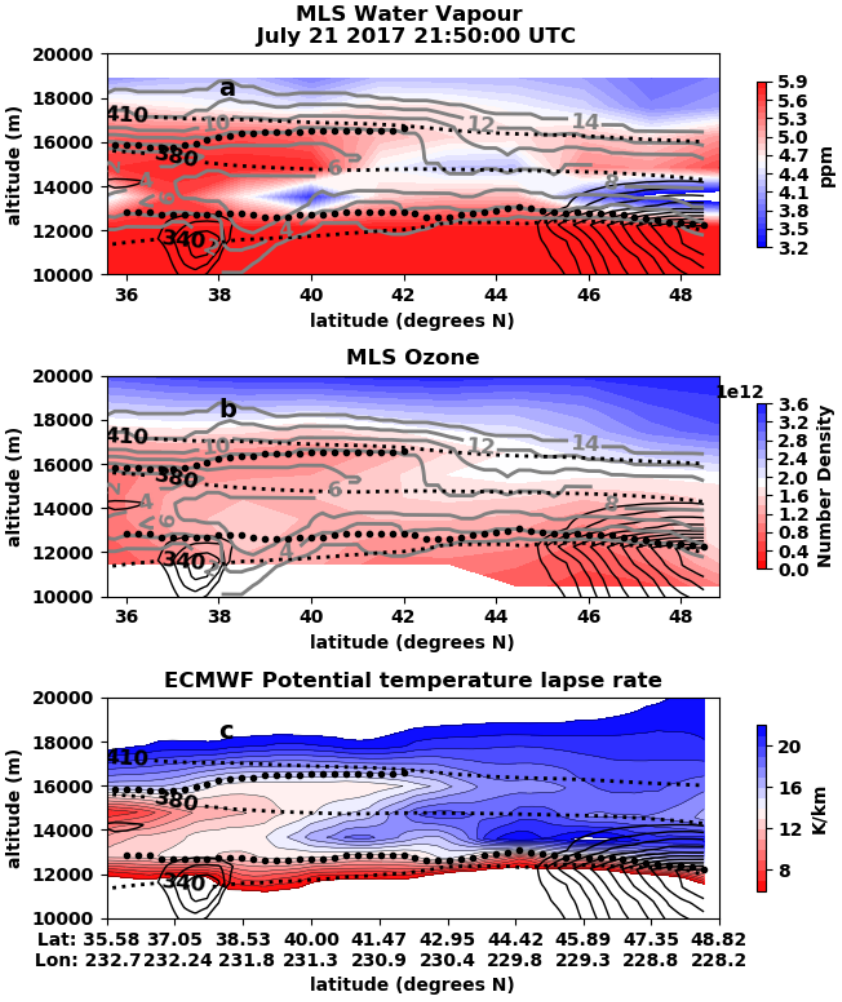

Figure 7 MLS measured water vapour profile (a), ozone (b) and the potential temperature lapse rate determined from the ECMWF reanalysis for the 22:00 UTC time step along the MLS measurement track (c).

The spatial structures recorded by SHOW (Figure 35) and MLS (Figure 46) during this intrusion event are strikingly similar and are consistent with spatial structures in the meteorological fields. A direct comparison shows that both instruments recorded similar amounts of water vapour in the vicinity of the subtropical jet. They both capture the moist filament near 16 km, as well as, the dry regions near 13.5 km in the lower latitude portion of the measurement tracks. The measurements are not expected to have exact agreement since the MLS measurements are made along a flight track that samples a slightly different region of the atmosphere. Also, the limb viewing geometry from a satellite is different from the aircraft and the MLS measurements have a lower vertical resolution (3-5 km) compared to the SHOW measurements (250 m). These differences introduce additional biases between the measurements that are difficult to quantify without an exact coincidence where retrieval averaging kernels could be used to compare more quantitatively although degrading of the SHOW measurements to MLS resolution is better left to a separate validation exercise. However, the coarser vertical resolution of MLS smears the vertical extent of the moist filament across a large vertical range of ~2 km.

Interestingly, the spatial structures observed in the MLS ozone and water vapour profiles are both shifted to a higher altitude relative to the PTLR and PV structures. The consistency of the shift between SHOW and MLS suggests a slight bias in the ECMWF reanalysis data; although, it is unclear exactly the cause of the bias. Regardless, it is clear that the spatial variability observed in the MLS ozone and water vapour measurements, in light of the higher resolution SHOW observations, is consistent with isentropic mixing and a tropospheric intrusion event associated withon the poleward side of the subtropical jet in the presence of a double tropopause.

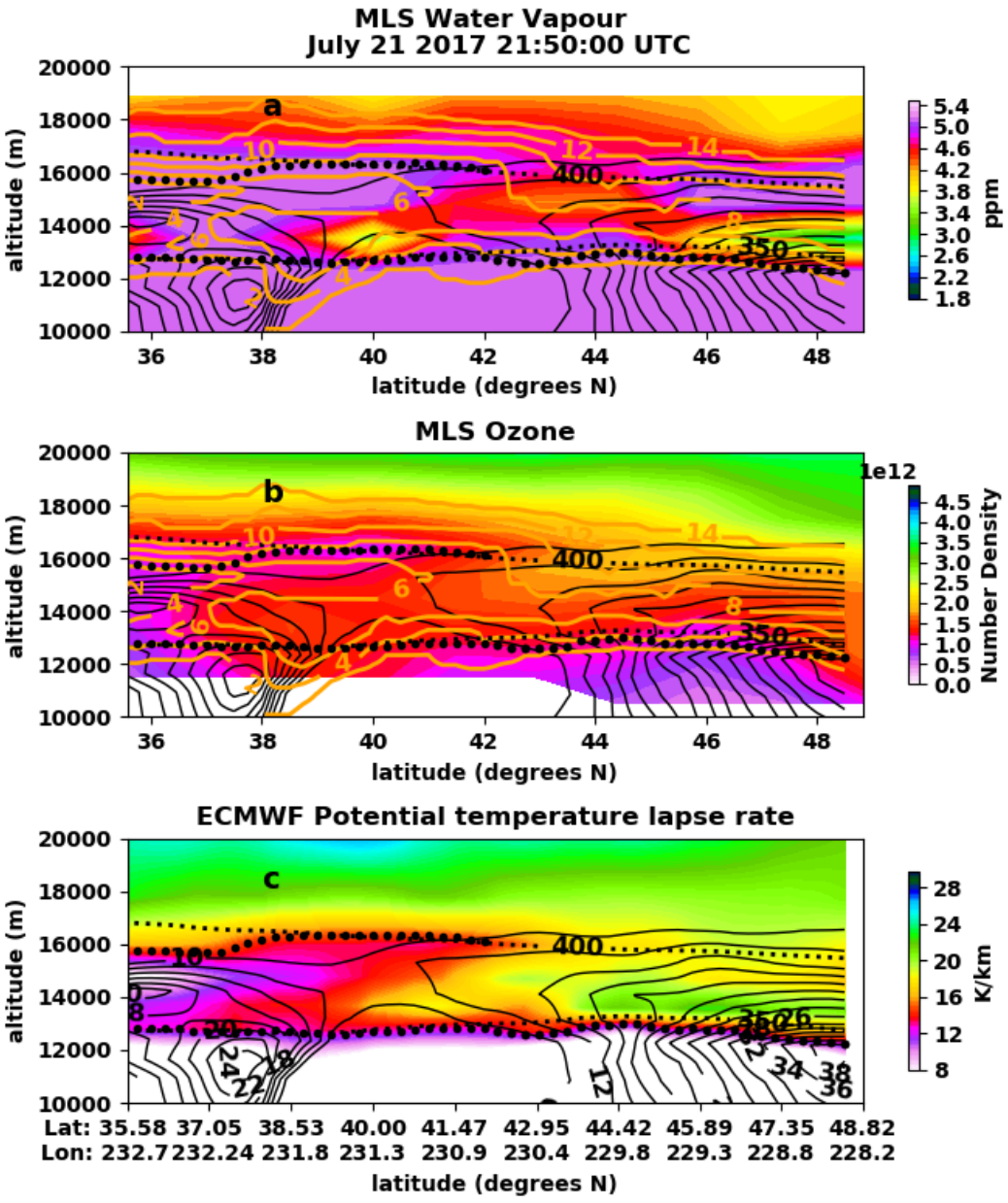

~~Figure 4 MLS measured water vapour profile (a), ozone (b) and the potential temperature lapse rate determined from the ECMWF reanalysis for the 22:00 UTC time step along the MLS measurement track (c).~~

475

6. Spatial extent of the event

To complete the picture it is prudent to examine the spatial extent of the suspected intrusion event. This is achieved by examining the PTLR at the 22:00 UTC time step in Figure 5(a) and Figure 5(b) for a longitude of 235.5 degrees and 230 degrees respectively. Latitudes from 30 degrees to 70 degrees North are shown to give a view of the larger dynamical picture. As before, the black contours show the zonal wind, the thick black dotted line shows the location of the thermal tropopause and the light black dotted lines show the 350 K and 400 K isentropes.

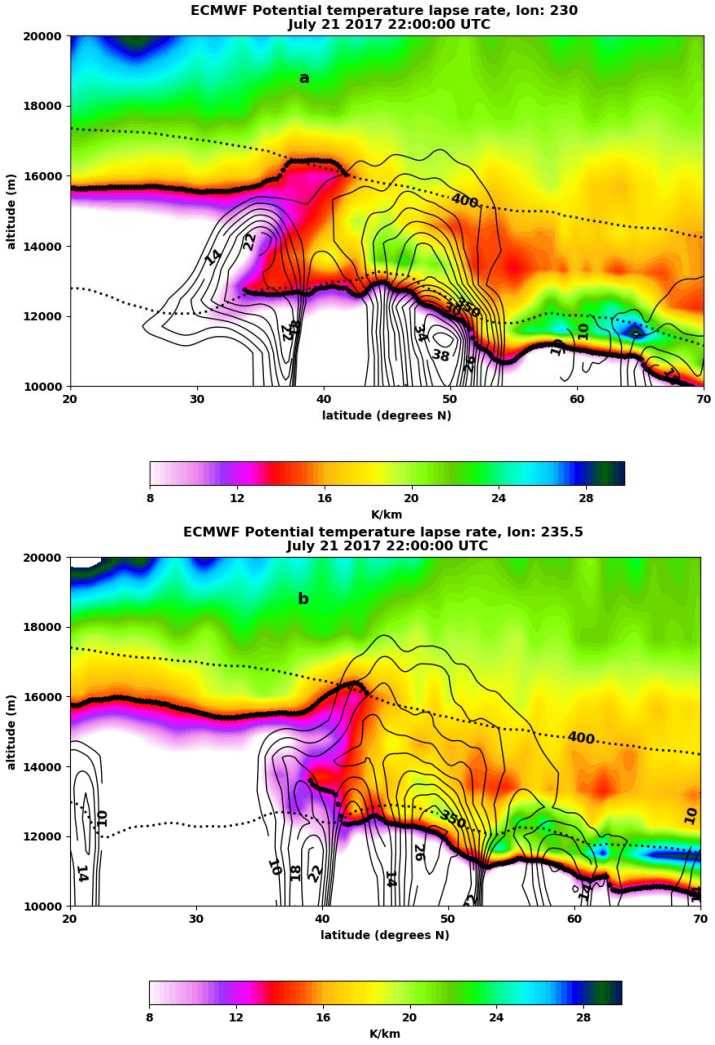

Figure 5 ECMWF calculated potential temperature lapse rate along the 235.5 and 230 degree longitude line determined from the ECMWF meteorological data at the 22:00 UTC time step

Along the 235.5 degree longitude (near the SHOW flight track) we see that the thermal tropopause is located close to 16 km below 39 degrees. Above 39 degrees, a double tropopause forms that extends

from 39 degrees North to 44 degrees North. On the other hand, for the 230 degree longitude (near the MLS flight track), the thermal tropopause sits close to 16 km below 33 degrees and the double tropopause extends from 32 degrees to 42 degrees. In both cases, the presence of the double tropopause coincides with a laminar structure that has PTLR < 12 K/km air that extends above and poleward of the jet. Only marginal differences are observed between the 19:00 UTC (Figure 3 (b)) and the 22:00 UTC time steps in the vicinity of the suspected intrusion.

The PTLR in the larger geographical region shows that the suspected intrusion and the associated double tropopause has a spatial extent that extends between 5-10 degrees poleward of the subtropical jet over the Pacific Ocean. The spatial structures observed in the measurements of water vapour with SHOW and ozone and water vapour with MLS act as tracers of this intrusion. In the SHOW measurements, the intrusion extends from 39.5 degrees to 43 degrees, whereas, in the MLS data, the intrusion extends over more than 10 degrees latitude.

7. Summary and Conclusion

In this paper we presented two-dimensional measurements of the water vapour distribution above and poleward of the subtropical jet. These measurements were obtained using the newly developed SHOW instrument during a sub-orbital demonstration flight on board NASA'S high altitude ER-2 airplane on July 21, 2017. The high spatial resolution sampling provided by SHOW revealed a moist filament that coincided with a double tropopause on the poleward side of the subtropical jet. Nearly coincident measurements of water vapour and ozone obtained using the AURA-MLS instrument recorded spatial structures that were consistent with the SHOW observations. However, it was shown that the vertical resolution provided by SHOW reveals fine spatial structure that is not revealed by the MLS measurements and is not captured in the metrological fields of the reanalysis model output. Therefore, the SHOW measurements provide additional insight into the mechanisms that are responsible for the observed mixing between the air masses.

Analysis of the water vapour distribution indicates that the observed moist filament is the result of isentropic mixing across and above the subtropical jet. The observed variability suggests a complicated mixing layer in the vicinity of the subtropical jet and supports the suggestion that tropospheric intrusions in the vicinity of a double tropopause are a potentially significant mechanism responsible for moistening the lower stratosphere.

6. Discussions and Conclusions

The SHOW measurements presented in this paper reveal fine spatial structures with vertical scales < 1 km in the two-dimensional water vapour profile near the subtropical jet. The meteorological picture that was presented in Section 2 indicates that these structures are associated with isentropic transport and mixing due to the "stirring" of a Rossby wave breaking event in the days leading up to the flight. The high vertical resolution measurements of the two-dimensional water vapour distribution provide a detailed window into the mixing processes that is not completely resolved in the reanalysis dynamical fields or the AURA MLS measurements.

The vertical resolution of the measurements determined from the full-width half maximum of the retrieval averaging kernel is 250 m and the precision on the measurements is < 0.3 ppm. The accuracy of the SHOW measurements and retrieval approach was examined in Langille et al., 2018 and was found to be < 0.5 ppm for a wide range of water vapour variability and background aerosol. The approximate line-of-sight accuracy of the SHOW observations determined from the flight data is < 150 m in the 13 km -18 km region. Comparison with collocated radiosonde measurements obtained during an Engineering flight on July 17, 2019 also showed excellent agreement [Langille et al., 2019]. This provides reasonable level of confidence that the variability observed in Figure 6 is reflective of the true state of the atmosphere at the time of measurement.

However, we must also note that the SHOW retrieval is sensitive to the upper and lower cut-off of the retrieval. In this paper, the upper boundary was chosen to be roughly 2 km below the aircraft altitude. Above this level, the sensitivity to water vapour is significantly reduced as the path between the aircraft and tangent point decreases. On the other hand, the lower boundary was chosen to be several km below the lapse rate tropopause at the beginning of the measurements. Below this level, the optical depth becomes too large to accurately retrieve water vapour information [see Langille et al., 2018. Ideally, this lower cutoff would actively chosen to track changes in the altitude of the lapse rate tropopause and allow retrievals several km below this altitude; however, the retrieval run was performed without a-priori knowledge of the meteorological picture. An active determination is also under development that utilizes the sensitivity of the Jacobian to changes in the water vapour profile to determine the appropriate cut-off [Langille et al., 2018]. In this paper, the lower boundary cut-off was fixed at 13.5 km using knowledge obtained from simulated retrievals in order to ensure the retrieval was not influenced by this effect.

The objective of the comparisons with the reanalysis data, as well as AURA MLS observations, is to identify the dynamical process that produced the measured water vapour structure. A number of factors can contribute to the differences and the offset displayed in the comparison. The reanalysis data has a vertical resolution of 1-3 km in the UTLS region. Therefore, the reanalysis data set has been used to confirm that the observed variability is consistent with general meteorological picture and isentropic mixing associated with Rossby wave breaking near the subtropical jet. On the other hand, the MLS measurements provide a means to confirm consistency with the large scale spatial variability; although, the measurements are not expected to have exact agreement since the MLS measurements are made

along a flight track that samples a slightly different region of the atmosphere. Also, the limb viewing geometry from a satellite is different from the aircraft and the AURA MLS measurements have a lower vertical resolution (1.3-3.2 km) compared to the SHOW measurements (250 m). The overall consistency supports the process identification despite the specific difference.

In conclusion, the high-spatial resolution measurements of a two-dimensional structure of the water vapour transport above and poleward of the subtropical jet provide unprecedented details of isentropic mixing across the tropopause break driven by Rossby wave breaking. The observed significant enhancement of water vapour in the lowermost stratosphere indicates that this type of transport is a significant process for stratospheric water vapour budget. The fine structure of the water vapour in the mixing process supports the importance of the high-resolution water vapour measurement capability. These measurements also serve to demonstrate the capabilities of the SHOW instrument and further advance the technical readiness of the instrument for future satellite deployment.

8.7. References

1 ~~Appenzeller,~~Añel, J. A., Antuña, J. C., De La Torre, L., Castanheira, J. M. and ~~Davies, H.C.: Structure~~Gimeno, L.: Climatological features of ~~stratospheric intrusions into the troposphere, Nature, 358, 570–572, 1992.~~

21 ~~Birner, T.: Fine-scale structure of the extratropical~~global multiple tropopause ~~region~~events, J. Geophys. Res~~., 111, D04104, https://~~. Atmos., doi~~.org/10.1029/2005JD006301, 2006~~:10.1029/2007JD009697, 2008.

2 ~~Brewer, A. W.: Evidence for a world circulation provided by the measurements of helium~~Banerjee, A., Chiodo, G., Previdi, M., Ponater, M., Conley, A. J. and Polvani, L. M.: Stratospheric water vapour ~~distribution~~: an important climate feedback, Clim. Dyn., doi:10.1007/s00382-019-04721-4, 2019.

3 Chen, P.: Isentropic cross-tropopause mass exchange in the extratropics, J. Geophys. Res.,~~stratosphere, Q.J.R. Meteorol. Soc., 75: 351-363,~~ doi:10.~~1002/qj.49707532603, 1949.~~1029/95jd01264, 1995.

4 Dessler, A. E., Hintsa, E. J., Weinstock, E. M., Anderson, J. G~~.,~~. and Chan, K. R.: Mechanisms controlling water ~~vapor~~vapour in the lower stratosphere: "A tale of two stratospheres~~",~~," J. Geophys. Res. Atmos., 100(D11), 23167–23172, ~~https://~~doi~~.org/~~:10.1029/95JD02455, 1995.

5 Dessler, A. E., ~~Dobson, G.~~Schoeberl, M. ~~B.: Origin~~R., Wang, T., Davis, S. M. and ~~distribution of the polyatomic molecules in the atmosphere. Proc. Roy. Soc. London, 236A, 187–193, https://doi.org/10.1098/rspa.1956.0127, 1956.~~

65 ~~Forster, P. M. de F., and Shine~~Rosenlof, K. ~~P~~H.: Stratospheric water vapour feedback, Proc. Natl. Acad. Sci. U. S. A., ~~vapor~~doi:10.1073/pnas.1310344110, 2013~~ changes as a possible contributor to observed stratospheric cooling, Geophys. Res. Lett., 26, 3309–3312, 1999~~.

76 Forster, P. M. de F~~Forster, P. M. de F.,~~ and Shine, K. P.: Assessing the climate impact of trends in stratospheric water ~~vapor~~vapour, Geophys. Res. Lett., ~~29(6), https://~~doi~~.org/~~:10.1029/~~2001GL013909~~2001gl013909, 2002.

7 Forster, P. M. Stohl, A., Bonasoni, P., Cristofanelli, P., Collins, W., Feicher, J., Frank, A., Forster, C., Gerasopoulos, E., Gäggeler, H., James, P., Kentarchos, T., Kromp-Kolb, H., Krüger, B., Land, C., Meloen, J., Papayannis, A., Priller, A., Seibert, P., Sprenger, M., Roelofs, G.J., Scheel, H.E., Schnabel, C., Siegmund, P., Tobler, L., Trickl, T., Wernli, H., Wirth, V., Zanis, P., D. F. and Shine, K. P.: Stratospheric water vapour changes as a possible contributor to observed stratospheric cooling, Geophys. Res. Lett., doi:10.1029/1999GL010487, 1999.

8 Gettelman, A., Hegglin, M. I., Son, S. W., Kim, J., Fujiwara, M., Birner, T., Kremser, S., Rex, M., Añel, J. A., Akiyoshi, H., Austin, J., Bekki, S., Braesike, P., Brhl, C., Butchart, N., Chipperfield, M., Dameris, M., Dhomse, S., Garny, H., Hardiman, S. C., Jöckel, P., Kinnison, D. E., Lamarque, J. F., Mancini, E., Marchand, M., Michou, M., Morgenstern, O., Pawson, S., Pitari, G., Plummer, D., Pyle, J. A., Rozanov, E., Scinocca, J., Shepherd, T. G., Shibata, K., Smale, D., Teyssdre, H. and Tian, W.: Multimodel assessment of the upper troposphere and lower stratosphere: Tropics and global trends, J. Geophys. Res. Atmos., doi:10.1029/2009JD013638, 2010.

~~8 Hintsa, E. J., and Zerefos., C.: Stratosphere-troposphere exchange: A review, and what we have learned from STACCATO, J. Boering, K. A., Weinstock, E. MGeophys. Res., 108, 8516, https://doi.org/10.1029/2002JD002490, D12, 2003.~~

~~9 Gettelman, A. and Sobel, A.H.: Direct Diagnoses of Stratosphere–Troposphere Exchange. *J. Atmos. Sci.*, 57, 3–16, https://doi.org/10.1175/1520-0469(2000)057<0003:DDOSTE>2.0.CO;2, 2000.~~

~~10 Gettelman, A., Hoor, P., Pan, L.L, Randel, W.J., Hegglin, M.I., and Birner, T.: The extratropical upper troposphere and lower stratosphere, Rev. Geophys., 49, 2011.~~

~~11 Harlander, J. M.: Spatial heterodyne spectroscopy: Interferometric performance at any wavelength without scanning, Ph.D. thesis, University of Wisconsin-Madison, 1991.~~

9 ~~Hegglin, M. I., Plummer, D. A., Shepherd, T. G., Scinocca, J. F.~~, Anderson, J. G., ~~, Froidevaux,~~Gary, B. L., ~~Funke~~Pfister, L., Daube, B. C., Wofsy, S. C., ~~, Hurst, D., Rozanov,~~ Loewenstein, M., Podolske~~A., Urban~~, J. R., Margitan, J. J. ~~, von Clarmann, T~~and Bui, T. P.: Troposphere-to-stratosphere transport in the lowermost stratosphere from measurements of H2O, CO2, N2O and O3, Geophys. Res. Lett., doi:10.1029/98GL01797, 1998.

~~12~~10 Högberg, C., Lossow, S., Khosrawi, F., Bauer, R., Walker, K. A., Eriksson, P., Murtagh, D. P., Stiller, G. P., ~~A., Wang, H. J., Tegtmeier, S., and Weigel, K.: Vertical structure~~Steinwagner, J. and Zhang, Q.: The SPARC water vapour assessment II: Profile-to-profile and climatological comparisons of stratospheric ~~water vapour trends derived~~δd(H2O) observations from ~~merged~~ satellite ~~data, Nat. Geosci., 7, 768–776, 2014~~, Atmos. Chem. Phys., doi:10.5194/acp-19-2497-2019, 2019.

~~13~~11 Holton, J. R., Haynes, P. H., McIntyre, M. E., Douglass, A. R., Rood, R. B.~~,~~ and Pfister, L.: Stratosphere-troposphere exchange, Rev. Geophys., ~~33(4), 403–439, https://~~doi.~~org/~~:10.1029/95RG02097, 1995.

12 Homeyer, C. R., Bowman, K. P., Pan, L. L., Atlas, E. L., Gao, R. S. and Campos, T. L.: Dynamical and chemical characteristics of tropospheric intrusions observed during START08, J. Geophys. Res. Atmos., doi:10.1029/2010JD015098, 2011.

13 Kley, D., et al. (2000), SPARC assessment of upper tropospheric and stratospheric water vapour, WCRP 113,World Meteorol. Organ., Geneva, Switz.

14 Kunz, A., Holton J.Konopka, P., Müller, R. and Pan, L. L.: Dynamical tropopause based on isentropic potential vorticity gradients, J. Geophys. Res., 116(D1), D01110, doi:10.1029/2010JD014343, 2011.

15 Kunz, A., Pan, L. L., Konopka, P., Kinnison, D. E. and Tilmes, S.: Chemical and dynamical discontinuity at the extratropical tropopause based on START08 and WACCM analyses, J. Geophys. Res. Atmos., 116(D24), n/a-n/a, doi:10.1029/2011JD016686, 2011.

14 R., Lelieveld J.: Stratosphere-Troposphere Exchange and its role in the budget of tropospheric ozone. In: Crutzen P.J., Ramanathan V. (eds) Clouds, Chemistry and Climate. NATO ASI Series (I: Global Environmental Change), vol 35. Springer, Berlin, Heidelberg, 1996.

15 Hurst, D. F., Lambert, A., Read, W.G., Davis, S.M., Rosenlof, K.H., Hall, E.G., Jordan, A.F., and Oltmans, S.J.: Validation of Aura Microwave Limb Sounder stratospheric water vapour measurements by the NOAA frost point hygrometer, J. Geophys. Res. Atmos., 119, 1612–1625, https://doi.org/10.1002/2013JD020757, 2014.

16 Langille, J. A., Solheim, B., Bourassa, A., Degenstein, S., Brown, S., and Shepherd, G.G.: "Measurement of water vapour using an imaging field-widened spatial heterodyne spectrometer," Appl. Opt. 56, 4297-4308 (2017)

1716 Langille J.A., Letros, D., Zawada, D., Bourassa, A., Degenstein, D.,, and Solheim, B.: Spatial Heterodyne Observations of Water (SHOW) vapour in the upper troposphere and lower stratosphere from a high altitude airplaneaircraft: Modelling and sensitivity analysis, Journal of Quantitative Spectroscopy and Radiative Transfer,VolumeJ. Quant. Spectrosc. Radiat. Transf., 209,Pages 137–149,ISSN 0022-4073, https://doi.org/10.1016/j.jqsrt.2018.01.026, doi:10.1016/j.jqsrt.2018.01.026, 2018.

17 Langille, J. A., Solheim, B., Bourassa, A., Degenstein, D., Brown, S. and Shepherd, G. G.: Measurement of water vapour using an imaging field-widened spatial heterodyne spectrometer, Appl. Opt., 56(15), doi:10.1364/AO.56.004297, 2017.

18 Langille, J., Letros, D., Bourassa, A., Solheim, B., Degenstein, D., Dupont, F., Zawada, D.,, and Lloyd, N. D.: Spatial heterodyne observations of water (SHOW) from a high-altitude airplane: characterization, performance, and first results, Atmos. Meas. Tech., 12,(1), 431–455, https://doi.org/:10.5194/amt-12-431-2019, 2019.

19 Livesey, N. J., Read, W. G., Wagner, P. A., Froidevaux, L., Lambert, A., Manney, G. L., Hegglin,Valle, L. F. M. I., Daffer, W., Pumphrey, H. C., Santee, M. L., Ray, E. A., Pawson, S., Schwartz, M. J., Wang, S., Fuller, R. A., Jarnot, R. F., J., Boone, C.Knosp, B. W., Martinez, E. and Lay, R. R.: Earth Observing System (EOS) Aura Microwave Limb Sounder (MLS) version 4.2x level 2 data quality and description document., 2018.

1920 Nedoluha, G. E., Kiefer, M., Lossow, S., Michael Gomez, R., Kämpfer, N., Lainer, M., Forkman, P., Martin Christensen, O., Jin Oh, J., Hartogh, P., Anderson, J., Bramstedt, K., Dinelli, B. M., Garcia-Comas, M., Hervig, M., Murtagh, D., Froidevaux, L., Raspollini, PLivesey, N.J., Read, W. G., Rosenlof, K., Stiller, G. P. and Walker, K. A.: Jet characterization in the upper troposphere/lower stratosphere (UTLS): applications to climatology and transport studiesThe SPARC water vapour assessment II: Intercomparison of satellite and ground-based microwave measurements, Atmos. Chem. Phys., 11, 6115-6137, https://doi.org/:10.5194/acp-11-6115-2011, 201117-14543-2017, 2017.

20 Manney, G.L., M.I. Hegglin, W.H. Daffer, M.J. Schwartz, M.L. Santee, and Pawson, S.: Climatology of Upper Tropospheric–Lower Stratospheric (UTLS) Jets and Tropopauses in MERRA. *J. Climate*, 27, 3248–3271, https://doi.org/10.1175/JCLI-D-13-00243.1, 2014

21 Müller, R., Pan, L., Solomon, S., Randel, W., Lamarque, J. F., Hess, P., Gille, J., Chiou, E. W. and McCormick, M. P.: Hemispheric asymmetries and seasonal variations of the lowermost stratospheric water vapour and ozone derived from SAGE II data, J. Geophys. Res. Atmos., doi:10.1029/97jd02778, 1997.

21 Kunz, A., Hurst, D. F., Rolf, C., Krämer, M. and Riese, M.: The need for accurate long-term measurements of water vapor in the upper troposphere and lower stratosphere with global coverage. Earth's Future, 4: 25–32, https://doi.org/10.1002/2015EF000321, 2016.

22 Pan, L. L., Randel, W. J., Gille, J. C., Hall, W. D., Nardi, B., Massie, S., Yudin, V., Khosravi, R., Konopka, P., and Tarasick, D.: Tropospheric intrusions associated with the secondary tropopause, J. Geophys. Res., 114, D10302, https://doi.org/10.1029/2008JD011374,(D10), D10302, doi:10.1029/2008JD011374, 2009.

23 Randel, W.J. and Jensen, E.J.: Physical processes in the tropical tropopause layer and their roles in a changing climate", Nature Geoscience, 6,169–176, 2013.

2423 Randel, W. J., Seidel, D. J., and Pan, L. L.: Observational characteristics of double tropopauses, J. Geophys. Res., 112, D07309, https://. Atmos., doi.org/10.1029/2006JD007904,:10.1029/2006JD007904, 2007.

24 Ray, E. A., Moore, F. L., Elkins, J. W., Dutton, G. S., Fahey, D. W., Vömel, H., Oltmans, S. J. and Rosenlof, K. H.: Transport into the Northern Hemisphere lowermost stratosphere revealed by in situ tracer measurements, J. Geophys. Res. Atmos., doi:10.1029/1999JD900323, 1999.

25 Riese, M., Ploeger, F., Rap, A., Vogel, B., Konopka, P., Dameris, M. and Forster, P.: Impact of uncertainties in atmospheric mixing on simulated UTLS composition and related radiative effects, J. Geophys. Res. Atmos., 117(D16), n/a-n/a, doi:10.1029/2012JD017751, 2012.

26 Scott, R. K. and Cammas, J. P.: Wave breaking and mixing at the subtropical tropopause, J. Atmos. Sci., Randel, W.doi:10.1175/1520-0469(2002)059<2347:WBAMAT>2.0.CO;2, 2002.

25 J., F. Wu, and Forster, P.: The Extratropical Tropopause Inversion Layer: Global Observations with GPS Data, and a Radiative Forcing Mechanism. *J. Atmos*. Sci., 64, 4489–4496, https://doi.org/10.1175/2007JAS2412.1, 2007.

26 Rodgers, C.: Inverse Methods for Atmospheric Sounding: Theory and Practice, World Scientific Publishing, Singapore, 2000.

27 Seidel, D. J., and Randel, W. J.: Variability and trends in the global tropopause estimated from radiosonde data, *J. Geophys. Res*., 111, D21101, https://doi.org/10.1029/2006JD007363, 2006.

2827 Solomon, S., Rosenlof, K. H., Portmann, R. W., Daniel, J. S., Davis, S. M., Sanford, T. J., &. and Plattner, G. K.: Contributions of stratospheric water vapour to decadal changes in the rate of global warming., Science, 327(5970), 1219–1223. https://doi.org/10.1126/science.1182488, (80-.)., doi:10.1126/science.1182488, 2010.

29 Sherwood, S. C., Roca, R., Weckwerth, T.M and Andronova, N.G.: Tropospheric water vapour, convection, and climate,Rev. Geophys., 48, 2010.

30 Talbot, D., Moran, M.D., Bouchet, V., Crevier, L.P., Ménard, S., Kallaur, A.: Development of a New Canadian Operational Air Quality Forecast Model. In: Borrego C., Miranda A.I. Air Pollution Modeling and Its Application XIX. NATO Science for Peace and Security Series. Environmental Security. Springer, Dordrecht, Infrared Physics & Technology,Volume 36, Issue 4,1995,Pages 763-777,ISSN 1350-4495, 2008.

28 Ungermann, J., Pan, L. L., Kalicinsky, C., Olschewski, F., Knieling, P., Blank, J., Weigel, K., Guggenmoser, T., Stroh, F., Hoffmann, L. and Riese, M.: Filamentary structure in chemical tracer distributions near the subtropical jet following a wave breaking event. Atmospheric Chemistry and Physics,, Atmos. Chem. Phys., 13,(20), 10517–10534, https://doi.org/:10.5194/acp-13-10517-2013, 2013.

29 World Meteorological Organization (1957), Meteorology: A three dimensional science, WMO Bull., 6, 134– 138.

30 WMO, (1992). International Meteorological Vocabulary. WMO Technical Publication No. 182.